AN EXPERIMENTAL STUDY OF COUPLED THERMO-HYDRO BEHAVIOR IN UNSATURATED SOIL

BY

NICE KANEZA, E.I.T.

Presented to the Faculty of the Graduate School of
The University of Texas at Arlington

In Fulfillment of the Requirements for the Degree of

MASTER OF SCIENCE IN CIVIL ENGINEERING

THE UNIVERSITY OF TEXAS AT ARLINGTON

AUGUST, 2020

To God, My Family, and My Friends

ACKNOWLEDGEMENTS

I would like to express my sincere gratitude to Dr. Xinbao Yu, my academic advisor and supervisor, for entrusting me and giving me the opportunity to work on this research project. I am truly thankful to the members of my graduate committee, Dr. Laureano R. Hoyos and Dr. Md Sahadat Hossain, for the insights and time that have been given to me. I would also like to sincerely thank my colleagues Xuelin Wang and Gang Lei for directing me and enriching my knowledge of heat transfer in unsaturated soil during my research project. I would like to express my appreciation to my colleagues Dr. Shi He, Sandesh Gautam, Madiha Alshammry, Dheeraj Shrimali, Rinu Samuel, Burak Boluk, Omid Habibzadeh Bigdarvish, and Harshwardhan Sawaitul for guiding and assisting me with all the research work that I have conducted at the University of Texas at Arlington.

I am grateful for the Dwight David Eisenhower Transportation Fellowship Program (DDETFP), as well as the United States Department of Transportation (USDOT) and the Federal Highway Administration (FHWA) for supporting me financially during my research.

My deepest gratitude is due to God for His love, grace, and mercy in every single step. My warmest thanks to my parents, Callixte Muzungu and Agnes Mujawayezu, and my siblings Nicole Muhire, Santiana Munezero, and Hervé Niyongabo for their love and cheerfulness. I am also thankful to my friends Jean de Dieu Mubiligi, Mireille Ishimwe, Yves Rudaseswa, Dr. Elvis Ishimwe, Ange Twagirumukiza, Olivier Kwizera, Isabelle Ishimwe, Innocent Kanyandekwe, Fessaly Rudasingwa, Christelle Izabayo, Caleb Kwizera, Hope Byishimo, Gedeon, Irumva, and Honoré Murenzi for showing their support and warmth during my studies.

August 10, 2020

ABSTRACT

An Experimental Study of Coupled Thermo-Hydro Behavior in Unsaturated Soil

Nice Kaneza, E.I.T.

The University of Texas at Arlington

Supervising Professor: Dr. Xinbao Yu

Understanding unsaturated soils in response to the impact of temperature will better predict the performance of geo-structures that extract and inject underground heat. Previous studies have shown that heat and water in unsaturated soil affect the movement of each other and that thermal gradients are responsible for the migration of water and thermal properties. Therefore, it is essential to study the coupling behavior of thermal and hydraulic (TH) processes to analyze the distribution of moisture and thermal properties of unsaturated soil. These processes are transient and difficult to examine in the field. In addition, there is a lack of laboratory testing apparatus to measure the coupled TH processes under controlled true one-dimensional heating condition. This thesis presents a modified soil testing cell, which was previously developed for agricultural applications and showed well-controlled one-dimensional heating in the soil. This device was used to conduct laboratory experiments to assess the coupling behavior of TH processes of unsaturated soil.

Two sands were selected for the experiments and compacted in the soil testing cell, equipped with thermocouples, time domain reflectometry sensors, and thermo-time domain reflectometry sensors. Different temperature boundary conditions were then imposed on the soil testing cell to create thermal gradients in the unsaturated soil. The measuring devices recorded the temperature variations and waveforms of the apparent dielectric constant (K_a) and bulk electrical conductivity (EC_b) that were used to calculate the gravimetric water content (ω) of soil using the Topp's equation, One Step method, and a and b method. It was observed that ambient temperature interfered with the temperatures imposed by the heat exchangers of the soil testing cell, as steady-state temperature distributions displayed a concave downward temperature profile for the tested unsaturated soil, due to the lack of proper insulation and gravity for the ASTM fine sand. This modified soil cell had proved, however, the ability to maintain one-dimensional heat transfer in previous studies presented herein. It was also noticed that among the two selected sands, the Hazy Meadow Park soil, containing the greatest amount of fine particles, with a low initial gravimetric water content and subjected to a moderate thermal gradient, more properly displayed the phenomenon of coupled TH processes in unsaturated soil.

TABLE OF CONTENTS

LIST OF FIGURES

Figure Page

LIST OF TABLES

Table Page

CHAPTER I

INTRODUCTION

1.1 Overview

In geothermal applications, ground-source heat pumps (GSHP) are used as energy-efficient geothermal systems for heating and cooling buildings and bridges, as shown in Figures 1 and 2. GSHP systems consist of geothermal energy piles or borehole heat exchangers that transfer heat from the earth to the lower atmosphere and from the lower atmosphere to the earth. The energy pile systems are drilled shafts that are inserted vertically into the ground below 6 m (20 ft.), where the temperature varies between 10 and 16°C (50 and 60°F) (National Renewable Energy Laboratory and US Department of Energy). Hydronic pipes are installed in the borehole heat exchangers and circulate heat transfer fluid. The fluid used is typically water mixed with antifreeze agents. The energy piles are connected to a heat pump that compresses and distributes the extracted underground heat to desired buildings and bridges in the winter season and injects heat from buildings and bridges into the ground in the summer season.

Enhanced geothermal systems (EGS) are also another type of geothermal systems that uses geothermal energy to produce electricity in cold and warm regions. Water is injected into the ground at about tens of kilometers underground, stimulates fractures in hot dry rock (HDR), is heated and extracted as hot water or steam, and is circulated again as cool water back into the HDR and so forth. The generated renewable energy is clean and reliable, and currently constitutes around 10 percent of the overall electric capacity in the United States (Office of Energy Efficiency and Renewable Energy).

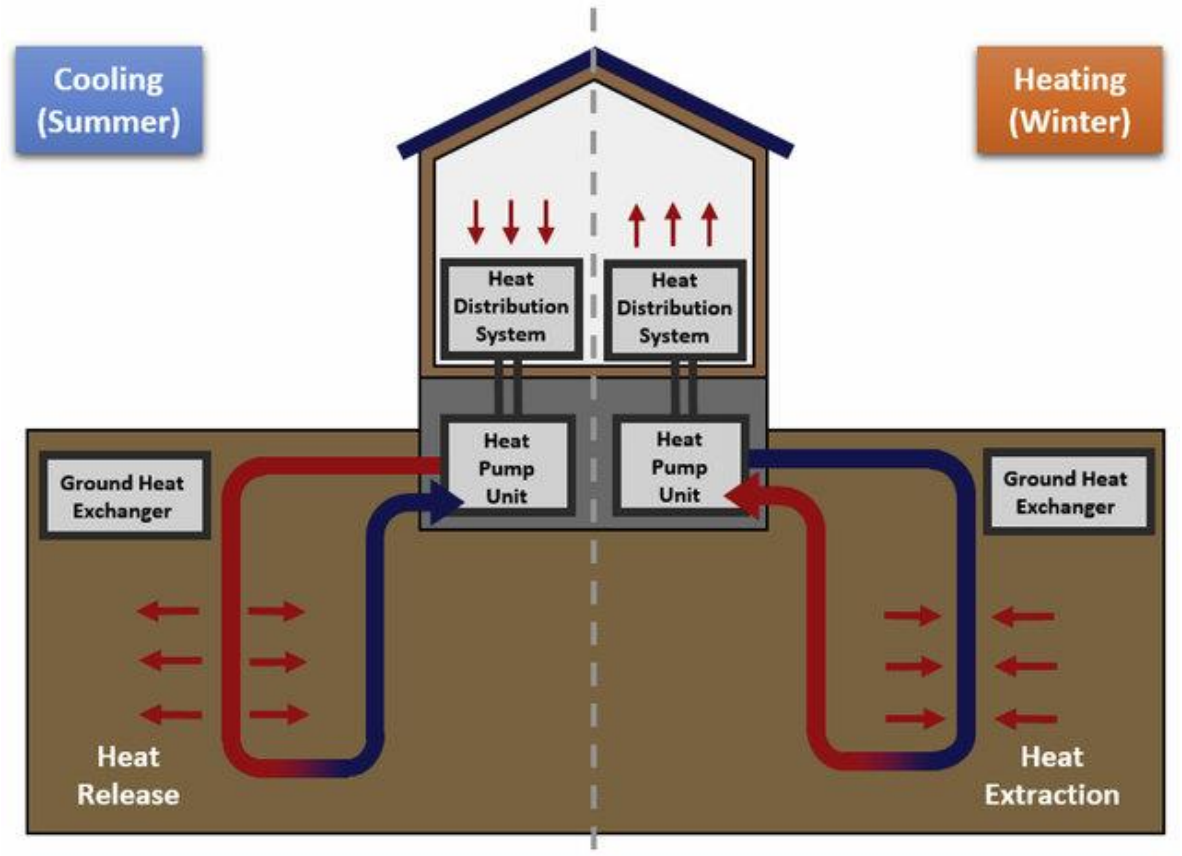

Figure 1. Structure of a ground source heat pump system.

The efficiency of the extraction and injection of heat depends partly on the temperature variations of the thermal interfaces between the pile/pipes and the surrounding soil, particularly soil layers above the water table or unsaturated soil (Fadejev et al. 2017; Xiao and Suleiman 2015; Shang et al., 2011). Unsaturated soil is a soil state that consists of solid soil particles, pore water, and pore air. When unsaturated soil is subjected to temperature changes, as a result of geothermal heat exchanges, the temperature gradients control the movement of water inside the soil pores. As the pore water moves, the temperature, thermal conductivity, and water suction in the soil are redistributed (Jackson, 1974; Cahill and Parlange, 1998). These processes are combined with other processes, including mechanical and chemical processes of unsaturated soil.

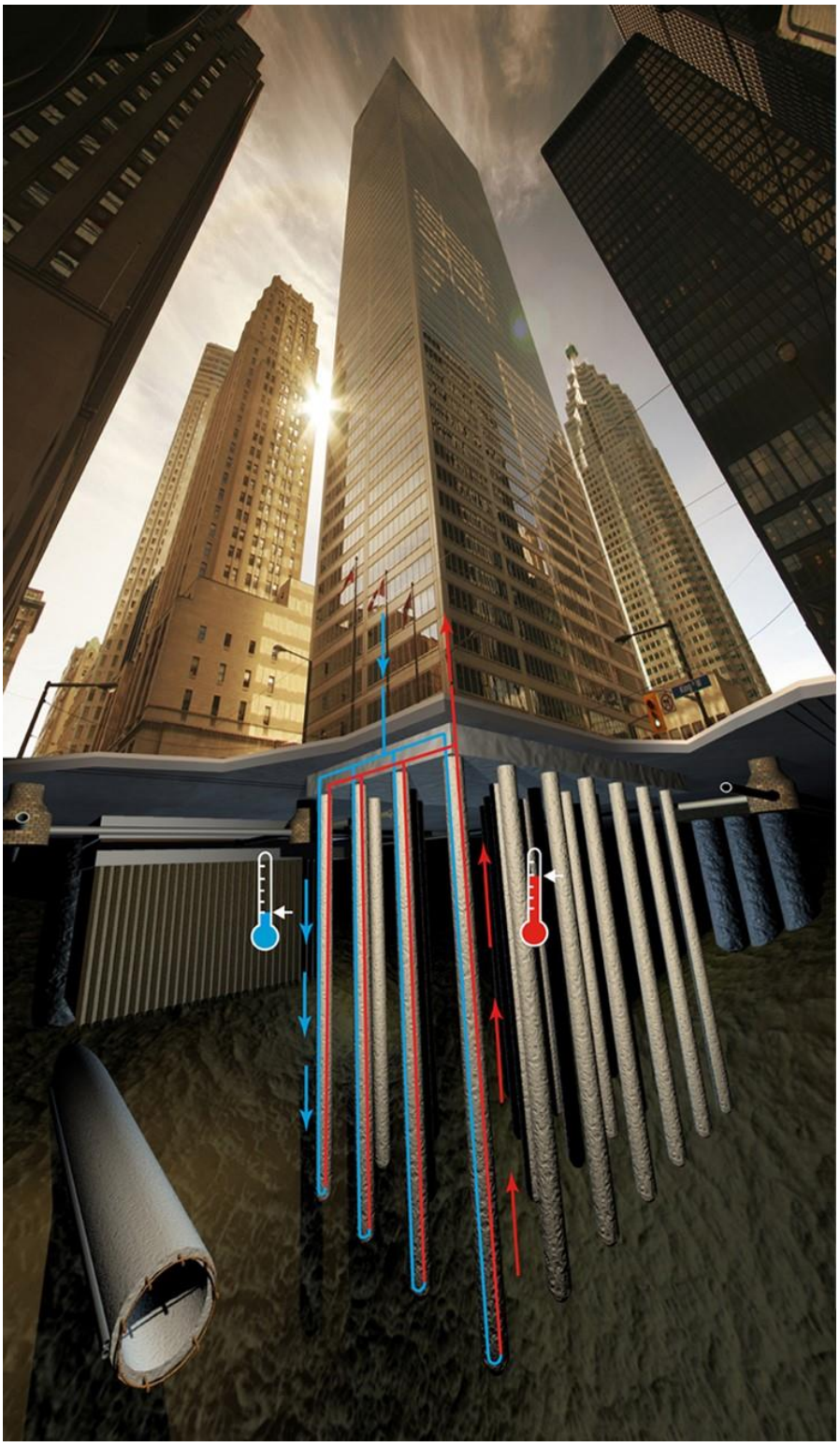

Figure 2. Heating and cooling of a geo-structure.

The combined mechanism of these processes is identified as coupled thermo-hydro-mechanical-chemical (THMC) processes and is critical for unsaturated soil (Wang and Wang 2003). The coupling behavior of these processes deals with several applications, namely the extraction and injection of geothermal energy, the function of ecosystem processes, and various aspects of agronomy (Agehara and Warncke, 2005; Shaver et al., 2006; Wennman and Katterer, 2006). Numerous studies on the THMC behavior of unsaturated soil have included both large-scale field tests and small-scale laboratory tests. The focus of this thesis is to evaluate the coupling of thermo-hydro (TH) processes by analyzing the interactions of the thermal and hydraulic properties of unsaturated soil on a small-scale in the laboratory.

In this study, to analyze the coupled TH phenomenon of unsaturated soil, experimental tests were performed in a laboratory setting using a modified double column-type testing device developed by Heitman et al. (2007). The soil testing cell was equipped with various sensors that measured the temperature, thermal properties, and moisture content of soil. One type of ungrounded silica sand and another sand retrieved from a park were selected for the laboratory experiments. This study provides advanced understanding of the coupled TH processes of unsaturated soil on a small scale.

1.2 Objective

The purpose of this study is to evaluate the coupled TH processes of unsaturated soil in a modified double column-type testing device in the laboratory. This objective was achieved in two phases. The first phase (Phase I) was to evaluate the design of the modified soil testing device according to the one-dimensional heat transfer theory. Various temperature boundary conditions were set for the heat exchangers of the soil testing cell, and the temperature variations in the double

column cell were monitored, to inspect whether one-dimensional heat transfer was maintained during the experiments. In the second phase, the same temperature boundary conditions were established, and the temperature and moisture content of the investigated soils were evaluated.

1.3 Problem Statement

A scientific understanding of coupled TH processes in unsaturated soil is essential for geothermal energy extraction and injection and other applications. However, the distribution of soil thermal properties and moisture content in the field is transient and difficult to examine. Moreover, despite the importance of the coupling of TH processes, there is still no sufficient and adequate equipment to effectively study this coupled phenomenon in the laboratory. Theories have been developed to predict the movement of moisture and temperature under transient conditions, but only a few have been effective for accurately estimating water and temperature distributions.

1.4 Thesis Structure

This thesis is elaborated as follows.

In Chapter 2, a brief description of the heat transfer theory and one-dimensional heat transfer is introduced. In this chapter, a summary of previous research work associated with the coupled TH behavior in unsaturated soil is also proposed.

Chapter 3 discusses the design of the modified testing device developed to study the coupling behavior of TH processes. The different components of the testing device, their dimensions, and the instrumentation, and their calibration analysis, used to measure the thermal properties and unsaturated soil moisture content are explored. The material used in the laboratory investigations are detailed, as well. Finally, an overview of the analyses of one-dimensional heat

transfer and coupled TH behavior in the soil cell is presented.

Chapter 4 presents the results of the experimental analyses. Moreover, discussions regarding the obtained results are provided.

Finally, Chapter 5 provides a summary and conclusions of all the research work presented in the thesis. This chapter also includes a section of recommendations on ways to improve experimental analyses of the coupled TH behavior in the future.

A list of references of the cited research work is provided at the end of each chapter, where needed.

1.5 References

Agehara, S. and Warncke, D.D. (2005). "Soil Moisture and Temperature Effects on Nitrogen Release from Organic Nitrogen Sources." Soil Science Society of America Journal, 69, 1844-1855. https://doi.org/10.2136/sssaj2004.0361

Cahill, A, and Parlange, M. (1998). "On Water Vapor Transport In Field Soils" 34 (4): 731–39.

Fadejev, J., Simson, R., Kurnitski, J., and Haghighat, F. (2017). "A Review on Energy Piles Design, Sizing and Modelling." Energy 122: 390–407. https://doi.org/10.1016/j.energy.2017.01.097.

Heitman, J. L., Horton, R., Ren, T. and Ochsner T. E. (2007). "An Improved Approach for Measurement of Coupled Heat and Water Transfer in Soil Cells." Soil Science Society of America Journal 71 (3): 872. https://doi.org/10.2136/sssaj2006.0327.

Jackson, R. D. (1974). "Diurnal Changes in Soil Water Content During Drying." https://doi.org/10.2136/sssaspecpub5.c3.

National Renewable Energy Laboratory. "Geothermal Energy Basics."

<https://www.nrel.gov/learning/re_geothermal.html>

Office of Energy Efficiency and Renewable Energy. "How an Enhanced Geothermal System Works." <https://www.energy.gov/eere/geothermal/how-enhanced-geothermal-system-works>

Shang, Y, Li, S., and Li, H. (2011). "Analysis of Geo-Temperature Recovery under Intermittent Operation of Ground-Source Heat Pump." Energy and Buildings 43 (4): 935–43. https://doi.org/10.1016/j.enbuild.2010.12.017.

Shaver, G. R., Giblin, A. E., Nadelhoffer, K. J., Thieler, K. K., Downs, M. R. Laundre, and J. A. Rastetter, E. B. (2006). "Carbon Turnover in Alaskan Tundra Soils: Effects of Organic Matter Quality, Temperature, Moisture, and Fertilizer." Journal of Ecology. 94 740–53.

US Department of Energy. "Geothermal Technologies Program: Geothermal Basics." <https://www.energy.gov/eere/geothermal/geothermal-energy-us-department-energy>

Wang, S. and Wang E. (2010). "Recent Study of Coupled Processes in Geotechnical and Geoenvironmental Fields in China."

Wennman, P. and Kätterer, T. (2006). "Effects of Moisture and Temperature on Carbon and Nitrogen Mineralization in Mine Tailings Mixed with Sewage Sludge." Environmental Quality, 35 (4) (2006), pp. 1135-1141

Xiao, S, and Suleiman, M. (2015). "Investigation of Thermo-Mechanical Load Transfer (t-z Curves) Behavior of Soil-Energy Pile Interface Using Modified Borehole Shear Tests." 1658–67. https://doi.org/10.1061/9780784479087.150.

CHAPTER II

LITERATURE REVIEW

2.1 Introduction

This chapter provides a description of the terms that are going to be used throughout this thesis. The different types of heat transfer are briefly discussed herein. This section also reports a summary of the previous research studies associated with one-dimensional heat transfer theory and its application in the coupled thermo-hydro behavior of unsaturated soil. The main objective of this chapter is to provide an understanding regarding the different ways that have been used to accurately study the paired processes of temperature and moisture transfer in unsaturated soil and to present the design of a modified double column-type testing device developed by Zhou et al. (2006).

2.2 Heat Transfer

In non-isothermal conditions, energy transfers from one region of higher temperature to another of lower temperature. It is the temperature gradient of the two regions that causes the movement of this energy. This energy is known as heat, and its flow is called heat transfer (Rohsenow et al., 1985). The amount of heat that is transmitted can be measured in terms of heat flux, which is the heat transfer rate per unit area normal to the direction of heat flow (Rohsenow et al., 1985). The heat transfer can occur between a solid and a liquid, a solid and a gas, and a liquid and a gas, or between two solids, two liquids, and two gases. There are three different modes of heat transfer: conduction, convection, and radiation (Kreith et al., 2010).

Heat conduction occurs when a solid, liquid, or gas medium of higher temperature enters in contact with another of lower temperature, and heat flows from the former to the latter. This transfer is caused by the collision of molecules; the molecules of the higher-temperature medium move at a higher speed and those of the lower-temperature medium at a lower speed. This transfer of energy is the heat conduction (Kreith et al., 2010).

The exchange of heat that takes place when a fluid, either liquid or gas, is heated is called the heat convection. The portion of the fluid that is warmer and lighter (less dense), due to its higher temperature, rises up to the top, and the portion that is cooler sinks to the bottom, because it is denser than the warmer portion of the fluid. This circulation pattern prevails until the fluid reaches equilibrium, and this mechanism is called the heat convection (Kreith et al., 2010).

Thermal radiation is the third form of heat transfer. Unlike the thermal conduction and convection, which require contact of the media that exchange heat, thermal radiation is transmitted without contact. A medium (solid, liquid, or gas) of higher temperature emits electromagnetic radiation and the medium of lower temperature absorbs it, until the two reach thermal equilibrium. The mechanism of electromagnetic radiation occurs at any temperature when the molecules of a warmer medium are vibrating and rotating at a faster rate than the neighboring cooler medium (Kreith et al., 2010).

There are simplified equations (Fourrier's law) (Kreith et al., 2010) that represent the thermal conduction, convection, and radiation, respectively, and they are described below. In this study, the mechanisms of conduction and convection are the focus of our analysis. Thereby, when unsaturated soil is heated, the solid soil particles transmit heat to the soil pore water through conduction, and warm pore water transmits heat to cool pore water through convection.

$$q" = -\frac{k}{dx}(T_2 - T_1) \quad (2\text{-}1)$$

$$q" = h(T_2 - T_1) \quad (2\text{-}2)$$

$$q = \sigma A_1({T_1}^4 - {T_2}^4) \quad (2\text{-}3)$$

Where q" is the heat flux in W/m^2; k is the thermal conductivity in W/m·k; T_i is the temperature of medium i in K; dx is the distance difference of two media; h is the local heat transfer in W/m^2K; q is the heat transfer rate in W; σ, which is equal to 5.669×10^{-8}, is the Stefan-Boltzmann radiation constant in $W/m^2 \cdot K^4$; and A is the heat transfer area of the medium in m^2.

2.3 Coupled Thermo-Hydro Processes

In geotechnical engineering and geo-environmental engineering applications, thermal properties and hydraulic properties of pore water of unsaturated soil are closely correlated. Heat transfer and water transport processes in unsaturated soil mutually interact with each other. Unsaturated soil is a porous medium that consists of solid soil particles and pores filled with water and air. In non-isothermal conditions, heat exchange from one region to another region within the soil lead to pore water movement. When the water moves, it transports the heat, and, in response, the thermal properties of unsaturated soil change. There are other interactions involved in this mechanism, such as the mechanical processes and chemical processes. The pairing of these interactions gives rise to a combined mechanism called coupled thermo-hydro-mechanical-chemical (THMC) processes (Wang and Wang, 2003).

This coupled phenomenon requires a unified analysis and cannot be studied individually, because each process influence the others at some degree (Tsang, Stephanson, Kautsky, 2005). Some research studies center their attention to the coupling of only two or three of these processes

– thermo-hydro (TH), thermo-mechanical (TM), hydro-mechanical (HM), thermo-hydro-mechanical (THM), and hydro-mechanical-chemical (HMC) – depending on the problem at geo-environmental or geotechnical circumstance. These circumstances include seepage and deformation of dam foundation and drainage and stability of slopes for the coupled HM processes; ventilation of underground excavation and frost or heat development in underground storage systems for the coupled TM processes; deep seated tunnel and mining and permafrost and freezing soil engineering for the coupled THM processes; chemical grouting in foundation treatment and ground pollution and treatment for the coupled HMC processes; and chemical mining and underground waste disposal for the coupled THMC processes (Wang and Wang, 2003).

As mentioned above, the analysis of particular processes of the coupling behavior depends upon the geotechnical and geo-environmental concern. Since this study analyzes the mechanism of coupled heat and water processes in unsaturated soil surrounding geo-structures, only the coupling of TH processes will be the ultimate focus of this research report.

In early 1910, researches have been conducted to study the movement of soil water in the field. Bouyoucous (1915) developed two separate wooden boxes, each containing cold water (0°C) and warm water (20 and 40°C), and placed 20.3-cm high and 3.8-cm wide columns consisting of various types of soil with different moisture content in the boxes. The soil columns were put in brass tubes and laid in the wooden boxes horizontally and vertically, and one half of the soil column was placed in the wooden box containing cold water, while the other half was placed in the warm water wooden box. Ice and warm water were added regularly to the wooden box for a total duration of 8 hours. This was done to create thermal gradients and to evaluate the movement of water in soil. At the end of the 8 hours, the two halves of the columns were placed into the oven to dry at 105°C for a period of approximately 24 hours. It was noticed that water in the soil had

migrated from the warm column to the cold column and that the amount of water transferred depended upon the initial moisture content and temperature gradients. The amount of water transferred increased with the initial soil moisture content until a certain initial moisture content was reached, then the movement of water started to decrease. The researcher concluded that the soil behavior was influenced by the laws of surface tension and viscosity of water in soil until the critical moisture content was attained; thereupon, the soil hydraulic processes were controlled by the strong attractive forces of soil for water. It was also noticed that for the highest temperature gradient (corresponding to temperature boundaries of 40 to 0°C), a greater amount of water was transfered from the warm to cold soil column.

The findings of Bouyoucous (1915) were corroborated by various authors, including Smith (1939, 1943), Winterkorn (1947), Gurr et al. (1952), Maclean and Gwatkin (1953), Taylor and Cavazza, (1954), Hatherly and Wood (1957), Kuzmak and Sereda (1957), Hutcheon (1958), Woodside and de Bruyn (1959), Taylor and Cary (1960), Jackson et al. (1965), Hoekstra (1966), and other recent investigators. They determined that the quantity of water migrating from warm to cool region is influenced mainly by the initial moisture content and magnitude of temperature gradients. They also suggested that this migration in unsaturated soil is due to the vapor pressure variations from warm to cool location in the soil.

The above-mentioned researchers conducted their experiments in the laboratory, whereas other investigators such as Rose (1968), Jackson et al. (1974), Westcot and Wierenga (1974), and Cahill and Parlange (1998) have performed their experimentation on a field-scale to study the coupling of TH behavior. Westcot and Wierenga (1974) quantified and developed a model to predict the vapor flux and heat transfer by measuring temperature and moisture variations in 7.6-cm diameter, 32-cm long sealed columns in a field setting. The soil columns were exposed against

daily temperature variations. They observed a consistency in the predicted and measured moisture and temperature distributions and confirmed the findings Rose (1968) and Jackson (1973) regarding the notable alterations in moisture content near soil surface, when the soil columns are subjected to daily temperatures.

Although there have been many successful research studies that evaluated the coupled temperature and water transfer processes (sometimes associated with other processes) in the field, the experiments have proven to be very challenging and particularly time-consuming. The investigations involved advanced test design and equipment, as well as painstaking interpretation of findings (Alonso and Alcoverro, 2004; Datta et al., 2004; Chijimatsu et al., 2004).

To counter these challenges, a need to study these processes on a smaller scale – laboratory – is more privileged. Various equipment have been used to analyze coupled TH processes in the laboratory, and one of the most successful testing devices is the soil column developed by Zhou et al. (2006). The researchers designed and tested four soil cell configurations different both in their diameters and lengths. The developed soil cell consisted of an inner column and an outer column and their dimensions were as follow: 20.0-cm long, 8.9-cm inner diameter, and 20.2-cm outer diameter (long wide); 20.0-cm long, 5.2-cm inner diameter, and 8.9-cm outer diameter (long narrow); 10.0-cm long, 8.9-cm inner diameter, and 20.2-cm outer diameter (short wide); 10.0-cm long, 5.2-cm inner diameter, and 8.9-cm outer diameter (short narrow). All the configurations also comprised an upper and a lower heat exchanger plate, in which a spiral path was chiseled out. Two copper plates were used to prevent the water in the spiral path from permeating the soil in the columns and also to uniformly distribute heat from the water in the spiral path to the tested soil.

The investigations performed determined that the short wide configuration of the soil cell

provided the most satisfactory results and that the soil in the outer column succeeded at limiting the ambient temperature interference, thus maintaining a one-dimensional temperature distribution. The short wide cell was later used by the same researchers to study the coupled TH processes of unsaturated soil. The test device was also equipped with instrumentation such as thermo-time domain reflectometry (T-TDR) sensors to measure the thermal properties and moisture variations under transient conditions. This approach advanced the studies of Bouyoucous (1915) and subsequent researchers who had faced limitations in collecting the moisture variations data only by destructive methods at the end of their experiments.

The test device developed by Zhou et al. (2006) was modified and equipped with new instrumentation, and is the subject of this study. The dimensions and structure of the modified soil cell are discussed thoroughly in Chapter III. Three (3) time domain reflectometry (TDR) sensors were utilized to measure the apparent dielectric constant (K_a) and bulk electrical conductivity (EC_b) of soil at three different heights. The small number of instrumentations in the soil cell reduces the risk of interference of the different sensors while recording the measurements. In addition, eight (8) type-T thermocouples were used to measure the temperature variations within the soil cell. Ottawa sand and Hazy Meadow Park soil were selected for the laboratory experiments, and various temperature boundary conditions were imposed. This study provides advances in the analysis of coupled TH processes of unsaturated soil on a small scale through a better approach of measuring soil temperature and moisture variations.

2.4 One-Dimensional Heat Transfer

Although many soil columns have been designed to study the coupled movement of temperature and moisture behavior in the laboratory, the study remains complex because the

analysis requires to maintain one-dimensional heat flow under transient conditions. Philip and de Vries (1957) established mathematical equations that govern the migration of water in porous media in the case of combined moisture and temperature gradients (2-4) and the conduction of heat in unsaturated soil (2-5).

$$\partial\theta/\partial t = \nabla \bullet (D_\theta \nabla\theta) + \nabla \bullet (D_T \nabla T) + \partial K/\partial z \quad (2\text{-}4)$$

$$C\, \partial T/\partial t = \nabla \bullet (\lambda \nabla T) + \rho L \nabla \bullet (D_{\theta vap} \nabla\theta) \quad (2\text{-}5)$$

Where θ is the volumetric moisture content in cm^3 of water/cm^3 of soil; t is time is sec; D_θ is the moisture diffusivity of soil in $cm^2\ sec^{-1}$; D_T is the thermal moisture diffusivity of soil in $cm^2\ sec^{-1}\ C^{-1}$; T is temperature in C; K is the hydraulic conductivity of soil in $cm\ sec^{-1}$; z is vertical ordinate in cm; C is the volumetric heat capacity of soil in $cal\ cm^{-3}\ C^{-1}$; λ is the thermal conductivity of soil in $cal\ sec^{-1}\ cm^{-1}\ C^{-1}$; ρ is the density of liquid water in g/cm^3; L is the latent heat of evaporation of water in $cal\ ^{g-1}$; and $D_{\theta vap}$ is the vapor moisture diffusivity of soil in $cm^2\ sec^{-1}$.

The findings of Philip and de Vries (1957) have been challenged by other recent investigators who have asserted that only a one-dimensional analysis could be performed using the developed equations. One-dimensional heat transfer is nonetheless difficult to attain in the laboratory. This complexity comes from the fact that, in the laboratory, the ambient temperature interferes with the imposed boundary temperature conditions set for the experiment. The axial temperature conditions imposed in the analysis are challenged by the ambient temperature that generates a radial temperature distribution. The water and heat in the soil is consequently redistributed, so as not to maintain one-dimensional heat distribution (Nassar and Horton, 1989; Bach, 1992).

Accordingly, soil columns were developed to analyze the one-dimensional heat transfer that satisfy with the one-dimension theory. Prunty and Horton (1994) designed a single cell column to study the processes of water and heat redistribution, but the outcome of the study did not satisfy the one-dimensional heat theory. The axial temperature distributions at steady-state were concave downward between the warm and cool end or top and bottom of the soil cells. The researches stated that the concave downward profile demonstrated the presence of ambient temperature interference, that thermal properties of unsaturated soil were non-linear, and that the temperature changes generated moisture movement.

More recently, Zhou et al. (2006) designed a new cell, which limited the non-linearity of thermal properties that was previously encountered. The cell consisted of two columns, an inner and outer column. The soil in the outer column was intended to serve as a buffer or dynamic insulation, so as to ensure a one-dimensional heat transfer in the inner column, under unsaturated conditions. They designed four soil cells with different sizes and established one optimal design that produced a concave upward distribution of temperature variations that indicates non-uniform thermal properties and one-dimensional heat transfer. This thesis presents a modified version of the short-wide soil cell designed by Zhou et al. (2006) and developed by Heitman et al. (2007). The details of the design are given in Chapter III.

2.5 Summary

This chapter reviews the different modes of heat transfer and how they apply in the evaluation of the TH processes. Two heat transfer modes, conduction and convection, are involved in the mechanism of the coupled TH processes. Several research studies pertaining to the behavior of the coupling of temperature and water transfer are presented. Some experiments were performed

on the field, whereas others were carried out in the laboratory. The latter alternative is preferred because it is economical and time efficient. Challenges, such as the interference of the ambient temperature, that are faced during the analysis of the coupled TH processes and ways to counter these challenges are also stated. A newly modified soil testing cell developed by previous researches is introduced. The new testing device was used to examine the moisture and temperature distributions in this study.

2.6 References

Alonso, Eduardo E., J. Alcoverro, F. Coste, L. Malinsky, V. Merrien-Soukatchoff, I. Kadiri, T. Nowak, et al. (2005). "The FEBEX Benchmark Test: Case Definition and Comparison of Modelling Approaches." International Journal of Rock Mechanics and Mining Sciences 42 (5-6 SPEC. ISS.): 611–38. https://doi.org/10.1016/j.ijrmms.2005.03.004.

Bach, L. (1992). "Soil water movement in response to temperature gradients: Experimental measurements and model evaluation." Soil Sci. Soc. Am. J. 56:37-46.

Bouyoucos, G.T. (1915). "Effect of temperature on the movement of water vapor and capillary moisture in soils." J. Agr. Res. 5:141-172.

Gurr, C.G., Marshall, T.J. and Hutton, J.T. (1952). "Movement of water in soil due to a temperature gradient." Soil Science, 74(5), pp.335-346.

Hatherly, L. W., and Wood, M. (1957). "Seasonal Variations in Subgrade Soil Moisture Content and Temperature with Depth in Bagdad, Iraq." Proceeding Fourth International Conference Soil Mechanics 2:114-119.

Heitman, J. L., Horton, R., Ren, T. and Ochsner T. E. (2007). "An Improved Approach for Measurement of Coupled Heat and Water Transfer in Soil Cells." Soil Science Society of America Journal 71 (3): 872. https://doi.org/10.2136/sssaj2006.0327.

Hoekstra, P. (1966). “Moisture Movement in Soils under Temperature Gradients with the Cold Side Temperature Below Freezing.” Water Res. Res. 2:241-250.

Hutcheon, W. L. (1958). “Moisture Flow Induced by Thermal Gradients with Unsaturated Soils.” Water and Its Conduction in Soils, Highway Research Board, Commission on Physico-Chemical Phenomena in Soils, Special Report No. 40, 113 p.

Jackson R. D., Reginato R. J., and van Bavel C. H. M. (1965). “Comparison of Measured and Calculated Hydraulic Conductivities of Unsaturated Soil.” Water Resour. Res. 1: 375-380.

Jackson, R. D., Rose, D. A., and Penman, H. L. (1965). “Circulation of Water in Soil under a Temperature Gradient.” Nature 205: 314-316

Jackson, R. D. (1973). “Diurnal Changes in Soil-Water Content During Drying.” Field Soil Water Regime. Soil Sci. Soc. Am. Proc. 37:505-509.

Kreith, F., Manglik, R. M. & Bohn, M. S. (2010). “Principles of heat transfer.” Cengage Learning, Stamford USA.

Kuzmak, J. M., and P. J. Sereda, P. J. (1957). “The Mechanism by Which Water Moves Through a Porous Material Subjected to a Temperature Gradient, I: Introduction of a Vapor Gap into a Saturated System.” Soil Science, 84:291-299.

Kuzmak, J. M., and P. J. Sereda, P. J. (1957). “The Mechanism by Which Water Moves Through a Porous Material Subjected to a Temperature Gradient, II: Salt Tracer and Streaming Potential to Defect Flow in the Liquid Phase.” Soil Science, 84:419-422.

Maclean, D. J. and Gwatkin, P. M. (1953). “Moisture Movements Occurring in Soil Due to the Existence of a Temperature Gradient.” Road Research Laboratory, Harmondsworth, Middlesex, England.

Nassar, I.N. and Horton, R. (1989). “Water transport in unsaturated nonisothermal salty soil: I.

Experimental results." Soil Sci. Soc. Am. J. 53:1323-1329.

Philip, J.R., and de Vries, D.A. (1957). "Moisture movement in porous materials under temperature gradients." Trans. Am. Geophys. Union 38:222-232.

Prunty, L. and Horton, R. (1994). "Steady-state temperature distribution in non-isothermal, unsaturated closed soil cells." Soil Sci. Soc. Am. J. 58:1358-1363.

Rohsenow W. M., Hartnett J. P. and Ganic E. N. (1985). Handbook of Heat Transfer Fundamentals, 2nd edn., Rohsenow W. M. et al. (Eds). New York.

Rose, C. W., Water transport in soil with a daily temperature wave, I, Theory and experiment, Aust. J. Soil Res., 6, 31-44, 1968a.

Rose,C . W., Water transport in soil with a daily temperature wave, I, Analysis, Aust. J. Soil Res., 6, 45-57, 1968b.

Smith, W. O. (1939). "Thermal Conductivities in Moist Soils." Proceeding of American Society Soil Science 4:32-40.

Smith, W. O. (1943). "Thermal Transfer of Moisture in Soils." Trans. Amer. Geophys. Union, 24, 511-524.

Taylor, S. A. and Cavazza, L. (1954). "The Movement of Soil Moisture in Response to Temperature Gradients." Soil Sci. Soc. Americ Proc. 18: 351-358.

Taylor, S. A. and Cary J. W. (1964). "Linear Equations for the Simultaneous Flow of Matter and Energy in a Continuous Soil System." Soil Sci. Soc, Amer. Proc. 28:167-172.

Tsang C, Stephansson O, Jing L, Kautsky F (2009) DECOVALEX Project from 1992-2007. Environ Geol 57:1221–1237.

Wang, S. and Wang, E. (2010). Recent Study of Coupled Processes in Geotechnical and Geoenvironmental Fields in China.

Wescot, D.W., and Wierenga, P.J. (1974). “Transfer of heat by conduction and vapor movement in a closed soil system.” Soil Sci. Soc. Am. Proc. 38:9-14.

Winterkorn, H. F. (1947). “Fundamental Similarities Between Electro-Osmotic and Thermo-Osmotic Phenomena.” Proc. Highway Res. Bd., 27, 443-454.

Woodside, W. and de Bryun, M. A. (1959). “Heat Transfer in a Moist Clay.” Soil Sci. Soc. 87:166-173.

Zhou, J., J. L. Heitman, R. Horton, T. Ren, T. E. Ochsner, L. Prunty, R. P. Ewing, and T. J. Sauer. 2006. “Method for Maintaining One-Dimensional Temperature Gradients in Unsaturated, Closed Soil Cells.” Soil Science Society of America Journal 70 (4): 1303. https://doi.org/10.2136/sssaj2005.0336n.

CHAPTER III

LABORATORY INVESTIGATIONS

3.1 Introduction

A new testing device was modified according to the design of the testing device developed by Zhou et al. (2006) and Heitman et al. (2007). The mentioned researchers designed and developed this testing device in order to establish one-dimensional heat transfer in a double column cell. Maintaining one-dimensional heat transfer is otherwise hard to attain in a laboratory setting, as discussed in the Literature Review section. The dimensions of the new testing device are slightly different from the previous devices. The cell also features another configuration and includes various instrumentations.

3.2 Design of a New Testing Device

Preliminary laboratory investigations were conducted to study the heat transfer in the modified double column cell (Lei et al., 2019, 2020). The cell consists of an inner column and an outer column. The two columns are both 101.6 mm (4 in.) high and 12.7 mm (0.5 in.) thick. The inside diameters of the inner column and the outer column are 88.90 mm (3.50 in.) and 209.55 mm (8.25 in.), respectively. Two heat exchanger plates were also included in the design. They are 25.4 mm (1.00 in.) thick each and have a diameter of 292.10 mm (11.50 in.). They incorporated an inner 6.5 mm x 6.5 mm (0.26 in. x 0.26 in.) spiral channel that circulates water in a 111.13 mm (4.38 in.) radius. In addition to the heat exchanger system is a copper plate, with a diameter of 292.10 mm (11.5 in.) and a thickness of 2.38 mm (3/32 in.). Two ring plates, as well as two O-rings, were used to attach the outer column to the heat exchanger plates. The heat exchangers have threaded holes that run through them to have a sealed cell. The columns, heat exchanger plates, and rings

are made of clear cast acrylic and were manufactured by Nationwide Plastics Inc. An illustration of the modified soil cell is provided below in Figures 3 and 4.

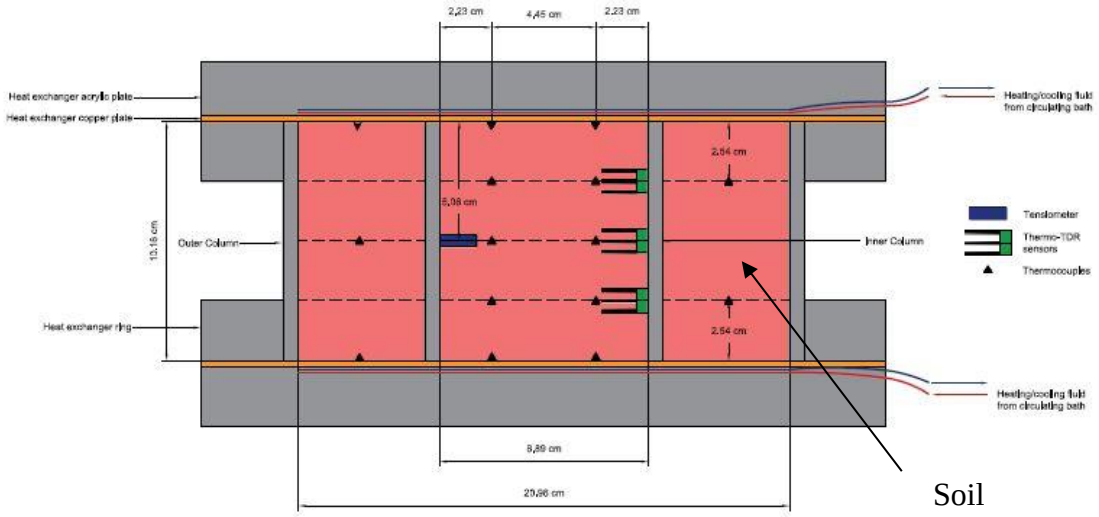

Figure 3. First configuration of the modified soil cell instrumented with T-TDR sensors and thermocouples.

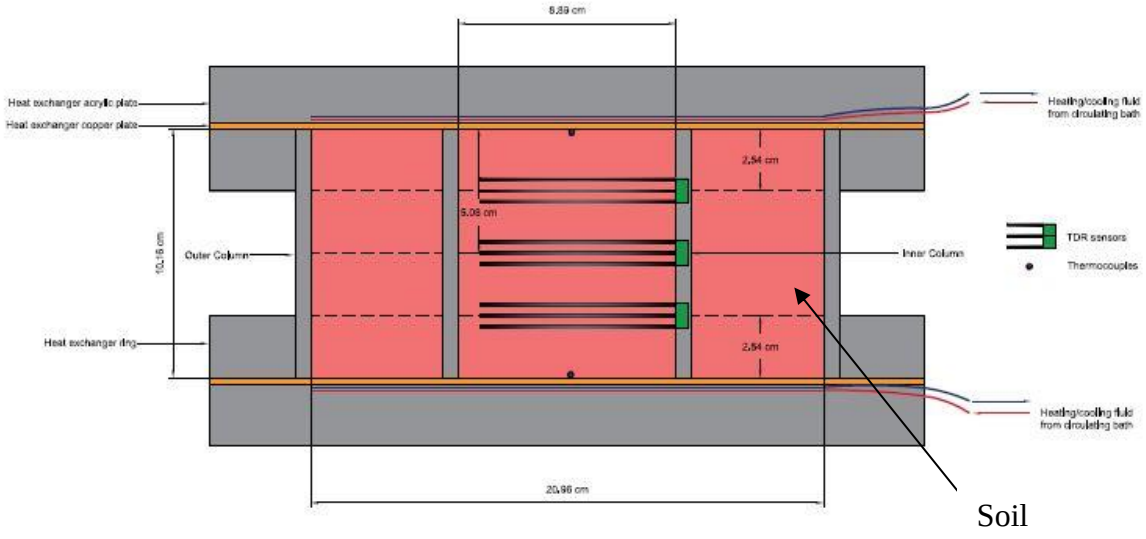

Figure 4. Second configuration of the modified soil cell instrumented with TDR sensors and thermocouples.

Warm and cool water was circulated from the temperature-controlled circulator (Model SD07R-20-A11B, PolyScience) to the heat exchangers and from a distance around the outer edge to the center of the heat exchangers, then returned from the opposite outer edge of the spiral channel to the circulator. A copper plate was installed between the heat exchanger and soil columns to uniformly distribute the water heat from warm water to the compacted soil.

3.3 Instrumentation

On one hand, the first configuration included fifteen (15) copper-constantan, Type T, thermocouples (TCs), which measured the temperature variations. The first ten (10) TCs were installed radially halfway between the wall and center of the inner column at the bottom (warm end) and top (cool end) of the cell and at positions of about 2.5, 5.0, and 7.5 cm along the axis of the inner cell, and the last five (5) TCs halfway were inserted at heights 0.0, 2.5, 5.0, 7.5, and 10 cm from either side between the inner and outer column walls.

The second configuration, on the other hand, included only eight (8) copper-constantan, Type T, thermocouples (TCs), shown in Figure 5, which measured the temperature variations. All the TCs were installed radially in the inner cell: six (6) of them halfway between the wall and center of the inner column at positions of about 2.5, 5.0, and 7.5 cm along the axis of the inner cell, and the remaining two (2) at the center of the warm and cool ends of the cell. The TDR sensors were installed radially at heights of about 2.5, 5.0, and 7.5 cm from warm end.

The design of thermocouples included a hypodermic stainless-steel needle from MicroGroup with specifications of 304 Hypo 14.5 Gauge 0.078” OD x 0.068” ID. A 2.54 cm long stainless steel tube was placed at the junction tip of the TCs. This tube allowed more contact area between the TCs and surrounding soil for greater accuracy in temperature measurements.

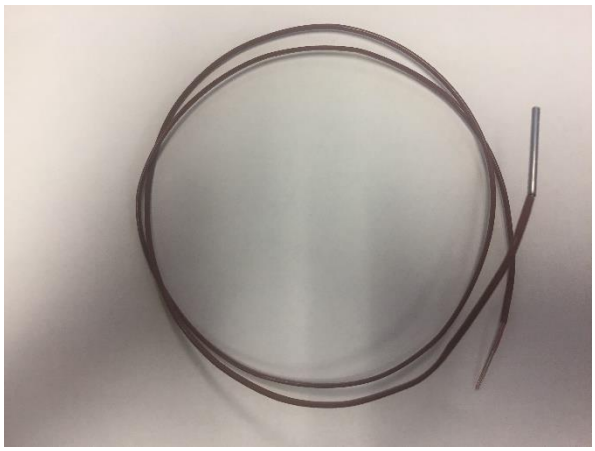

Figure 5. Type-T thermocouple with stainless-steel needle.

The first configuration comprised three (3) thermo-time domain reflectometry (thermo-TDR) sensors, which were used to measure the temperature, apparent dielectric constant (K_a), and thermal conductivity (λ) of soil specimens during the experiment, whereas the second configuration (Figures 6, 7, and 8) consisted of three (3) TDR sensors to measure the K_a and bulk electrical conductivity (EC_b). The former configuration was omitted, because it included too many measuring devices for such a small cell, and the used T-TDR sensors did not provide acceptable measurements of certain soil properties, as previously anticipated.

The thermocouples were manufactured by Omega Engineering Inc and adjusted by the author. TC-08 thermocouple data logger and PicoLog Recorder from PICO Technology and C Series Temperature Input Module and NI LabVIEW from National Instruments were used to measure and record the temperature variations, respectively. The TDR and thermo-TDR sensors were fabricated by Xuelin Wang and Nice Kaneza. The fabrication process of these sensors is briefly discussed in the Fabrication and Calibration of Sensors section and detailed by Yu et al. (2015). The K_a and EC_b waveforms were recorded by the TDR 100 soil moisture meter.

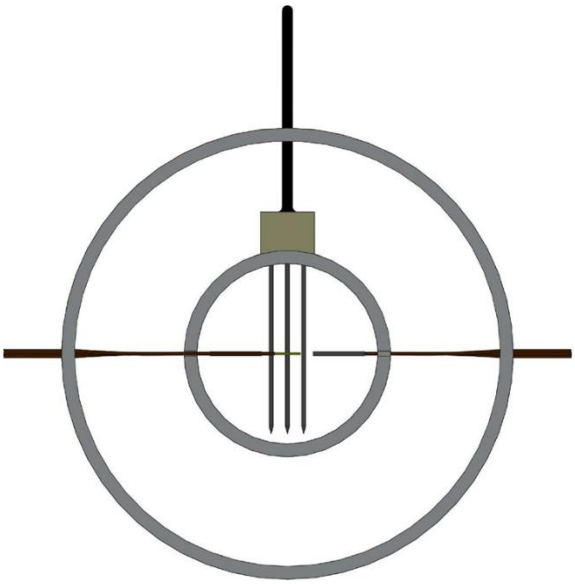

Figure 6. Plan view of the inner and outer cells instrumented with thermocouples and TDR sensors.

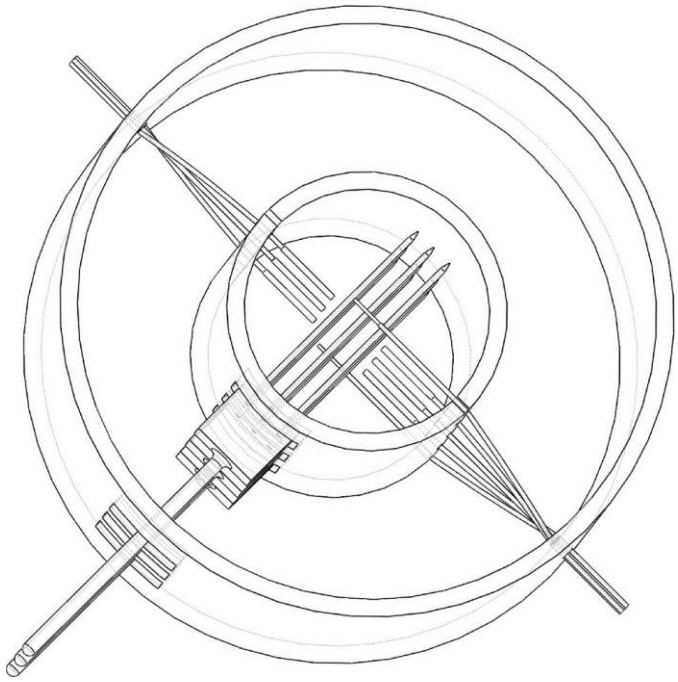

Figure 7. Isometric view of the inner and outer cells instrumented with thermocouples and TDR sensors.

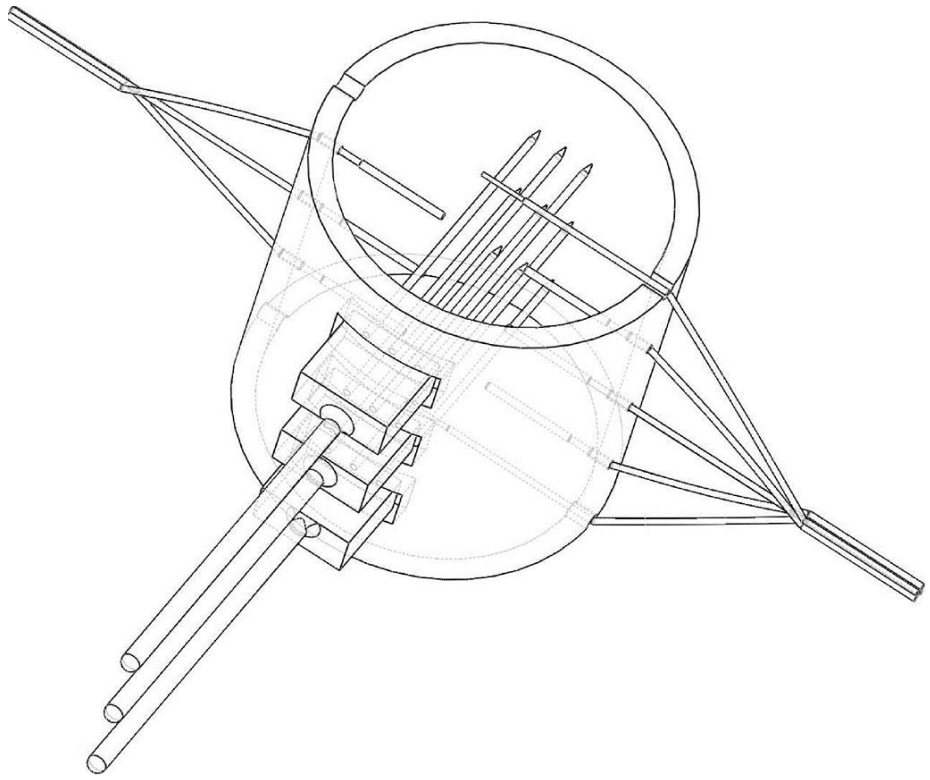

Figure 8. Isometric view of the inner cell instrumented with thermocouples and TDR sensors.

3.4 Fabrication and Calibration of Sensors

This section presents a series of time domain reflectometry and thermo-time domain reflectometry (TDR and T-TDR) sensors tests. It includes sensors fabrication and calibration test results for the K_a and EC_b of different chemical substances. The TDR and T-TDR sensors calibration was carried out for eight (8) sensors, namely TDR-1, TDR-2, TDR-3, TDR-4, T-TDR-1, T-TDR-2, T-TDR-3, and T-TDR-4, shown in Figures 9, 10, and 11.

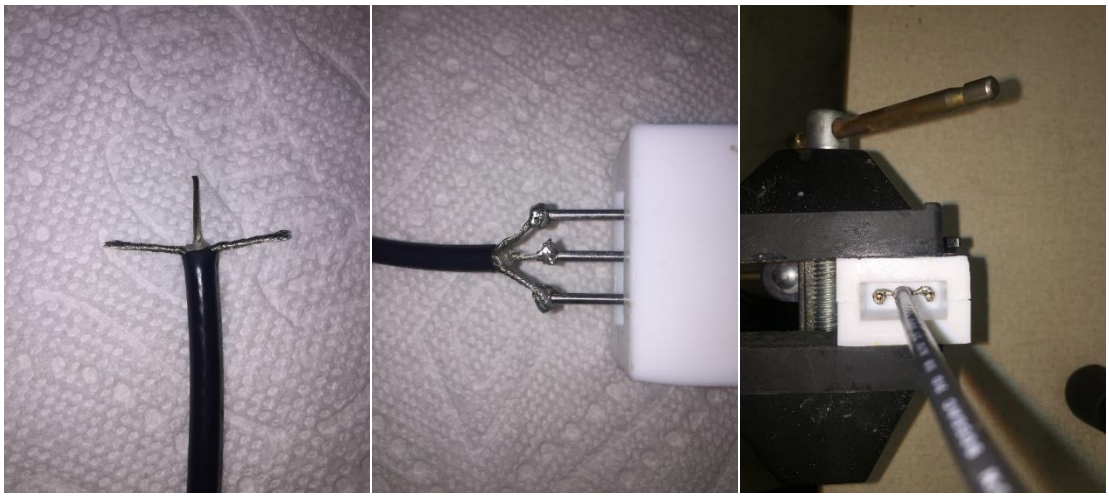

Figure 9. Fabrication process of the TDR sensors.

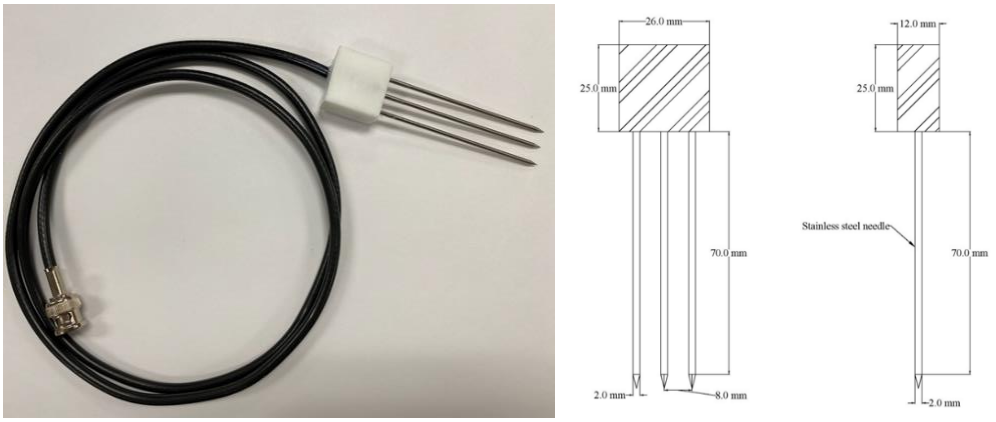

Figure 10. Complete assembly and schematic drawing of the TDR sensors.

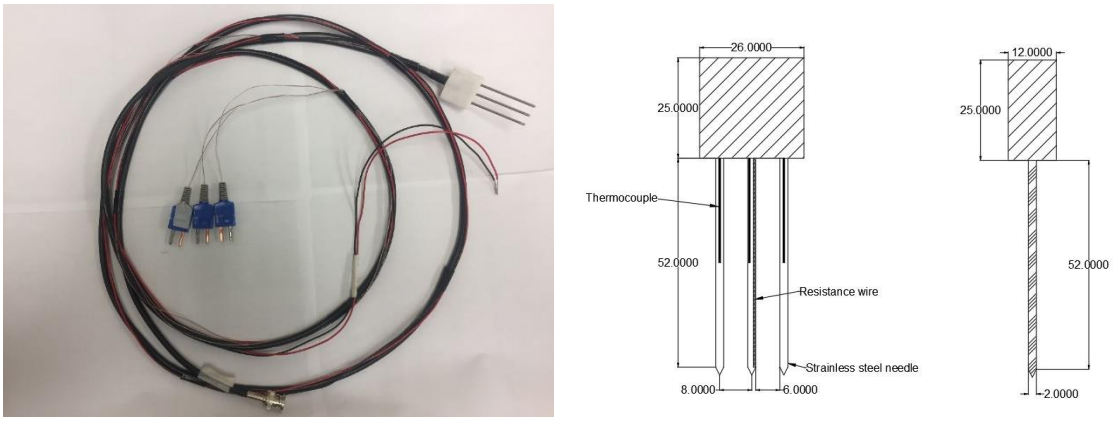

Figure 11. Complete assembly and schematic drawing of the T-TDR sensors.

The TDR and T-TDR sensors are integrated sensors that measure the water content of soil and simultaneously assess the thermal properties of the soil. All the sensors were fabricated in NH236 at University of Texas at Arlington under the guidance of Dr. Yu Xinbao, with the help of Xuelin Wang, Nice Kaneza, and Gang Lei. The sensors are composed of the items listed below:

- Hypodermic stainless-steel tubes from MicroGroup with specifications of 304 Hypo 14.5 Gauge 0.078" OD x 0.068" ID. The tube came in 5-feet length.
- Three Type-T precision fine wire thermocouples from Omega Engineering Inc. with wire diameter of 0.003" and Teflon insulation. The thermocouple wires were 36 inches long.
- 38-gauge Nichrome 80 resistance wire from Pelican Wire Company, Inc., which came in a spool of 50 feet length.
- 24 AWG conducting wires from Consolidated Electronic Wires & Cable.
- 50 ohms impedance coaxial cable from AlphaWire. (1.219 m for T1, 1.524 m for T2)
- CR-600 Casting Resin from Micro-Mark which came in 32 fluid ounce twin bottles.
- Thermal epoxy OMEGABOND 200 RESIN and MEGABOND 200 CATALYST from Omega Engineering Inc.

The K_a and EC_b of the selected sands were measured using the sensors in order to determine the water content of the soil. The following equations were used:

- **Apparent dielectric constant**

$$\boldsymbol{K_a}(-) = (L_a / L_p)^2 \qquad (3\text{-}1)$$

Where,

K_a = apparent dielectric constant

L_p = physical length of the probe in testing materials, m

L_a = apparent length (length on the waveform) of the probe in the testing materials, m

- **Bulk electrical conductivity**

$$\boldsymbol{EC_b}(Sm^{-1}) = \frac{\varepsilon_o c Z_o}{L_p Z_c}\left(\frac{2V_o}{V_f} - 1\right) \quad (3\text{-}2)$$

Where,

EC_b = bulk electrical conductivity

V_o = source voltage (V_o = 1.0 V)

V_f = long-term voltage level of reflected signal, V

ε_o = dielectric permittivity of free space ($\varepsilon_o = 8.85 \times 10^{-12}$ Fm^{-1})

c = speed of light in vacuum ($c = 3 \times 10^8$ m/s)

L_p = probe length, m

Z_o = characteristic probe impedance, which is 165.33 Ω

Z_c = TDR cable tester output impedance (Z_c = 50 Ω)

The sensors measure uncalibrated values of K_a and EC_b. To validate the measured values of the sensors, the TDR sensors were calibrated using different chemical substances with known K_a and EC_b values. The measured values were determined from the waveforms recorded by the TDR100 soil moisture meter. Standard and measured K_a values of the chemical substances are detailed in Tables 1, 2, and 3. The obtained calibration curves are illustrated in Figures 12 and 13.

Table 1. Standard and TDR measured apparent dielectric constant values of different chemical substances.

		TDR-1	TDR-2	TDR-3	TDR-4
Chemicals	**Actual dielectric constant, Ka_a**	**Measured dielectric constant, Ka_m**			
Air	1.00	0.60	0.65	0.77	0.65
Cyclohexane	2.02	2.09	1.67	1.88	1.60
Olive Oil	3.10	2.71	2.26	2.40	2.15
Castor Oil	4.70	3.36	2.64	2.74	2.32
Dichloromethane	8.93	8.36	7.63	8.03	7.78
Acetone	20.70	21.06	19.88	20.78	19.39
Methanol	32.70	33.05	31.30	31.74	29.49
Deionized water	80.10	78.47	78.28	78.09	76.27

Table 2. Standard and T-TDR measured apparent dielectric constant values of different chemical substances.

		T-TDR-1	T-TDR-2	T-TDR-3	T-TDR-4
Chemicals	**Actual dielectric constant, Ka_a**	**Measured dielectric constant, Ka_m**			
Air	1.00	0.74	0.81	0.86	-
Cyclohexane	2.02	2.50	1.50	2.17	-
Olive Oil	3.10	3.87	1.66	3.05	-
Castor Oil	4.70	4.70	2.98	3.24	-
Dichloromethane	8.93	10.38	8.04	9.34	8.86
Acetone	20.70	24.61	22.51	22.56	22.11
Methanol	32.70	34.15	25.83	39.12	25.43
Deionized water	80.10	90.67	82.42	93.44	86.89

Table 3. Equations of TDR and T-TDR sensors measured apparent dielectric constant.

Sensors	Equations	a	b	R^2
TDR-1	y = 1.0160x + 0.2454	1.0106	0.2454	0.9994
TDR-2	y = 1.0120x + 0.9003	1.0120	0.9003	0.9996
TDR-3	y = 1.0154x + 0.5711	1.0154	0.5711	0.9994
TDR-4	y = 1.0409x + 0.9855	1.0409	0.9855	0.9992
T-TDR-1	y = 0.8872x + 0.1236	0.8872	0.1236	0.9985
T-TDR-2	y = 0.9674x + 1.5300	0.9674	1.5300	0.9903
T-TDR-3	y = 0.8463x + 0.7709	0.8463	0.7709	0.9992
T-TDR-4	y = 0.8885x + 3.7793	0.8885	3.7793	0.9810

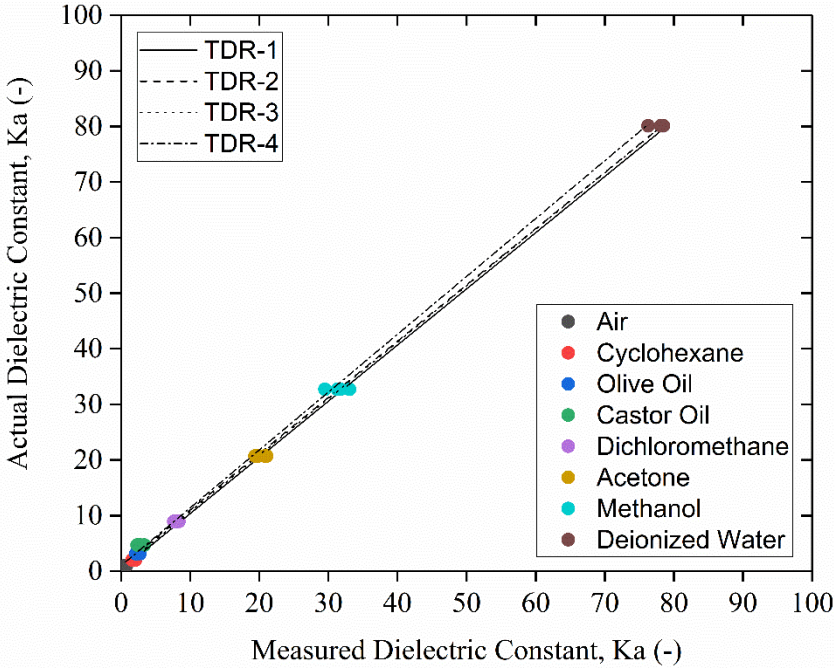

Figure 12. Apparent dielectric constant calibration curves of TDR sensors.

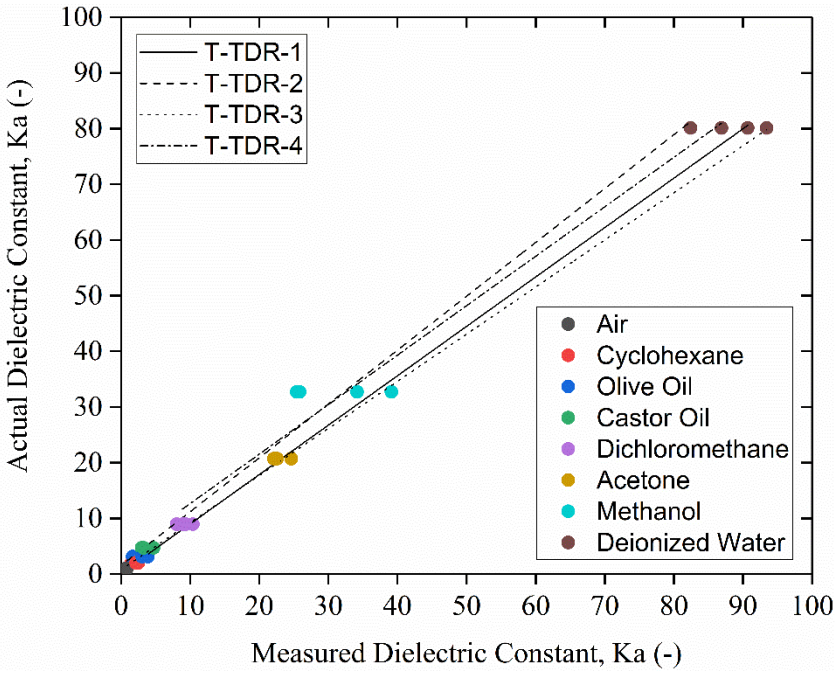

Figure 13. Apparent dielectric constant calibration curves of T-TDR sensors.

The calibration for the EC_b was performed using the solutions of sodium chloride (NaCl) and potassium chloride (KCl), with different concentrations ranging from 50 to 750 ppm, using both the TDR probes and the electrical conductivity meter (EC meter). The model of the hand-held EC meter is Oakton CON 6+. The calibration curves and equations obtained for EC_b are shown in Figures 14 and Table 4.

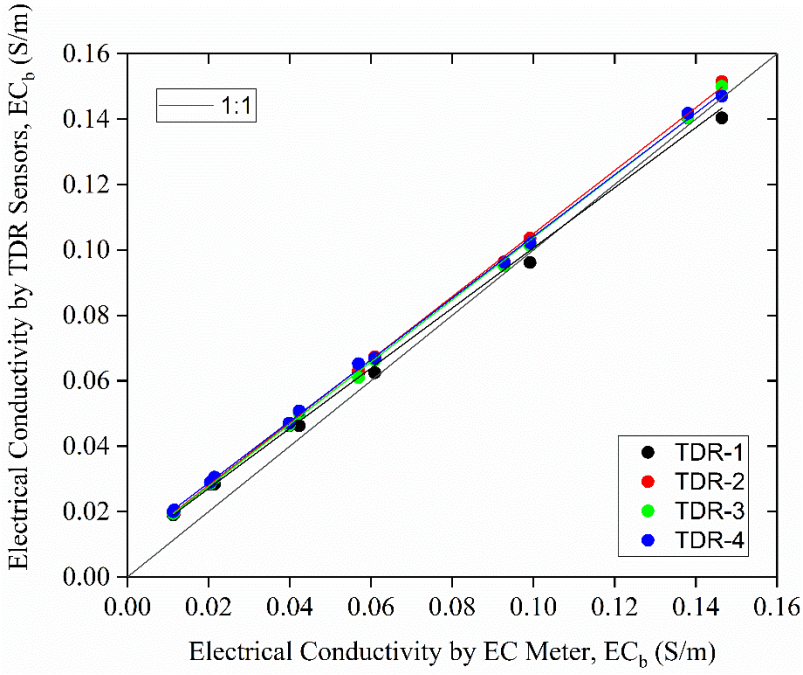

Figure 14. Bulk electrical conductivity calibration curves of TDR sensors.

Table 4. Equations for TDR sensors measured bulk electrical conductivity.

Sensors	Equations	a	b	R^2
TDR-1	y = 0.9197x + 0.0087	0.9197	0.0087	0.9971
TDR-2	y = 0.9628x + 0.0087	0.9628	0.0087	0.9996
TDR-3	y = 0.9514x + 0.0087	0.9514	0.0087	0.9993
TDR-4	y = 0.9425x + 0.0099	0.9425	0.0099	0.9995

3.5 Materials and Methods

Two soil samples were selected for the laboratory experiments: the American Society for Testing and Materials (ASTM) fine sand was retrieved from Ottawa, Illinois, and the Hazy Meadow Park soil was retrieved from Grapevine, Texas. Sieve analyses of both soil samples were performed, and gradation was determined and shown in Figure 15. The two soil samples have particle sizes ranging from approximately 0.150 mm to less than 1.00 mm for ASTM fine sand and less than 0.075 mm to less than 1.00 mm for the Hazy Meadow Park soil. The Hazy Meadow Park soil contains about 17 percent of fine particles.

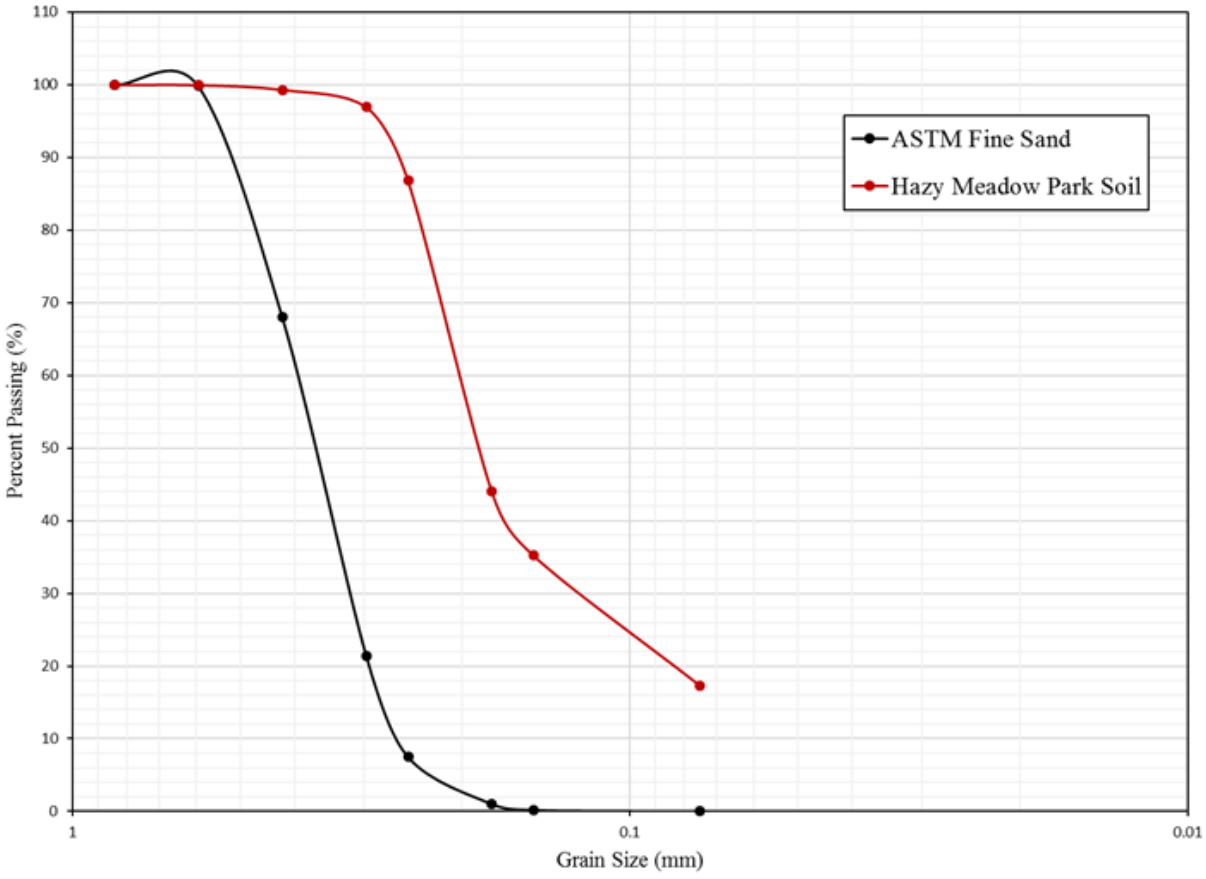

Figure 15. Particle size distribution of ASTM fine sand and Hazy Meadow Park soil.

The soil samples were dried in the oven at 105°C for 24 h and then mixed with the desired amount of distilled water prior to starting the test. Next, the soil was compacted into the inner column, then into the outer column, in four equal 2.54-cm layers for both columns. Compaction was carried out so as to achieve a dry density of 1.60 g/cm^3.

During the packing, the TCs and thermo-TDR/TDR sensors were installed in the soil cell and connected to the channels of the datalogger and soil moisture meter, as specified in the Instrumentation section. The sensors were connected to the soil moisture meter as shown in Figures 16, 17, and 18. Additionally, after compacting each layer, small soil samples were collected for oven-dried gravimetric water content determination.

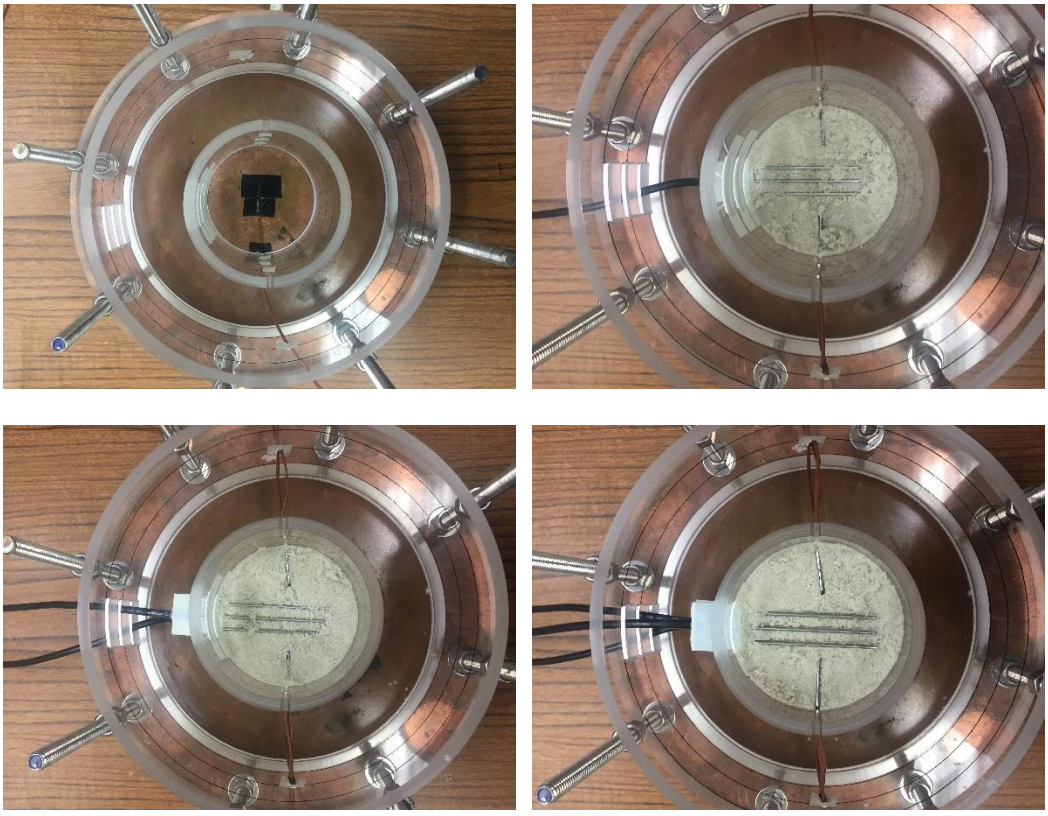

Figure 16. Compaction steps of ASTM fine sand in the modified soil cell.

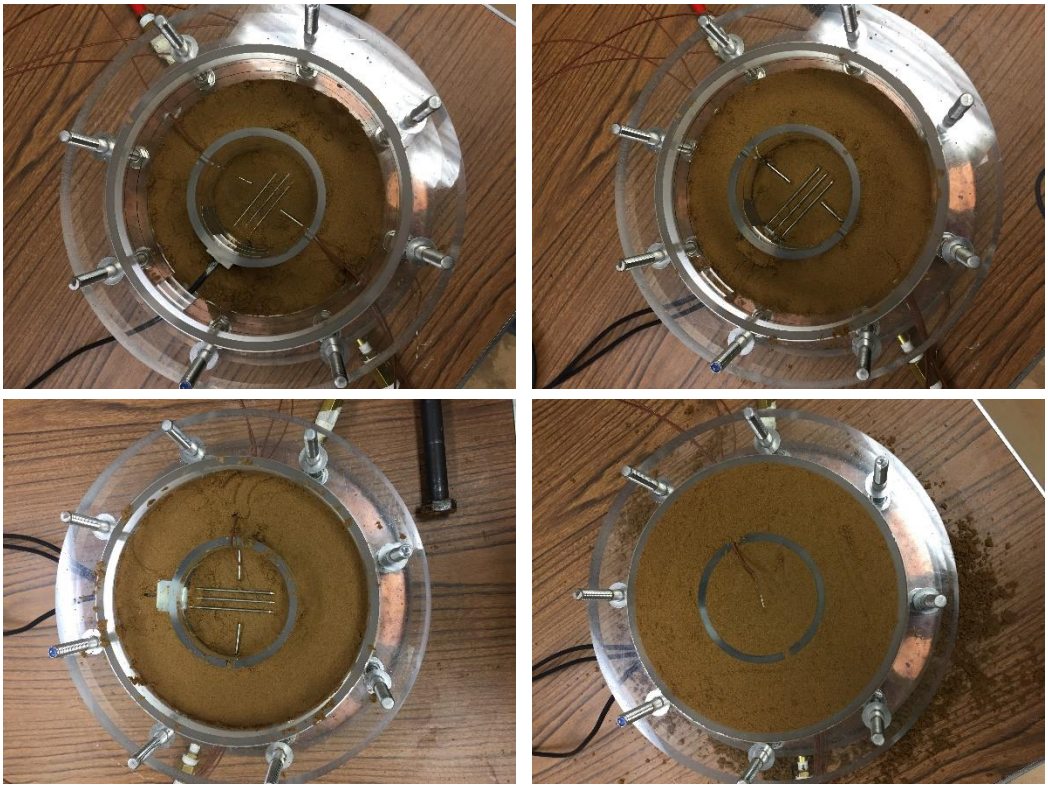

Figure 17. Compaction steps of Hazy Meadow Park soil in the modified soil cell.

Following the soil compaction, a heat exchanger was positioned at the top of the inner and outer cells so as to form a sealed soil cell. The water bath circulators were set to a temperature of 20°C to allow equilibrium in moisture distribution in the soil. At this time, the data loggers and soil moisture meter started recording the variations of temperature and K_a and EC_b waveforms within the soil testing cell. The room temperature was maintained at around 22°C. The temperature changes in the inner cell were recorded every minute during the heating and the TDR/thermo-TDR sensors recorded the K_a and EC_b waveforms at ten-minute interval. After a few hours, temperatures of 60°C and 40°C were imposed on the lower heat exchanger, for the ASTM fine sand and Hazy Meadow Park soil, respectively. The recording was stopped after approximately 48 h for the dry soil and 96 h for the moist soil after the heating started. The soil was then cooled down to 20°C

and additional samples were collected to measure the final oven-dried gravimetric water content.

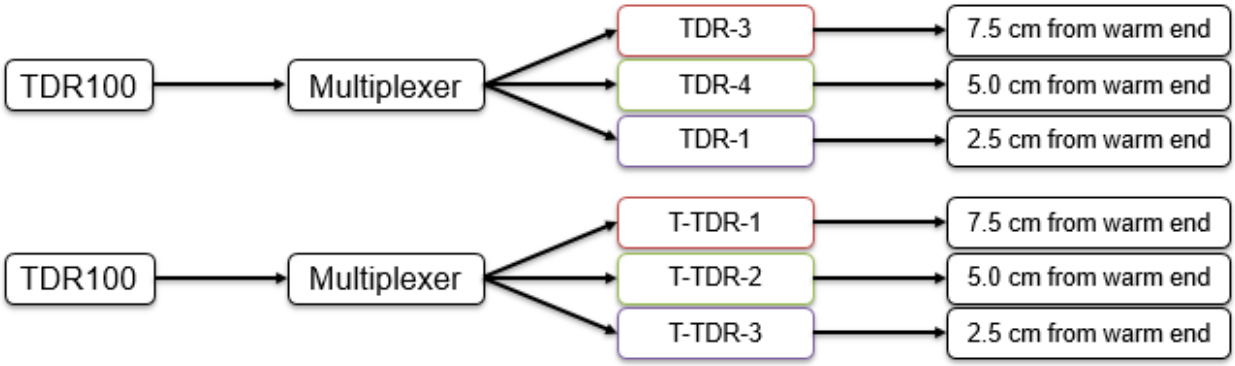

Figure 18. Sensors connection.

3.6 Experimental Plan

The laboratory experiments were performed according to the following the scope and test sequence.

Table 5. Scope

Test Name	Objective	Prospects
TH Behavior Test	Experimentally evaluate the temperature and water distributions	Coupling of the thermal and hydraulic processes of the tested soils

Table 6. Overview

Materials	Instrumentation	Function	Number and Placement
ASTM Graded Sand; Hazy Meadow Park Soil	Type-T Thermocouples	Measure the temperature variations	Eight (8) total; One (1) at the top and bottom and two (2) at 2.5, 5.0, and 7.5 cm from the bottom of the cell
	TDR sensors	Measure the dielectric constant and electrical conductivity	Three (3); at 2.5, 5.0, and 7.5 cm from the bottom of the cell

Table 7. Experimental Values

		Inner Column				Outer Column			
θ_{target} (m^3/m^3)	ω_{target} (%)	V_S (cm^3)	V_W (cm^3)	$m_{Dry\ Soil}$ (g)	m_w (g)	V_S (cm^3)	V_W (cm^3)	$m_{Dry\ Soil}$ (g)	m_w (g)
Using TDR sensors									
0	0	631	0	1010	0	2681	0	4290	0
0.096	6		60.6		60.6		257.4		257.4
0.160	10		101.0		101.0		429.0		429.0
Using T-TDR sensors									
0	0	631	0	1010	0	2681	0	4290	0
0.080	5		50.5		50.5		214.5		214.5
0.160	10		101.0		101.0		429.0		429.0
0.240	15		151.5		151.5		643.5		643.5
0.288	18		181.8		181.8		772.2		772.2

Table 8. Test Sequence

Tests	Soil	θ_{target}	ω_{target}	Boundary Conditions, T		Mean Temperature, T	Thermal Gradient, T
		(m^3/m^3)	(%)	(°C)		(°C)	(°C/m)
				Top	Bottom		
		Using TDR Sensors					
Coupled TH Behavior	ASTM Fine Sand	0	0	20	60	40	400
	ASTM Fine Sand	0.096	6	20	60	40	400
	ASTM Fine Sand	0.160	10	20	60	40	400
	Hazy Meadow Park Soil	0	0	20	40	30	200
	Hazy Meadow Park Soil	0.096	6	20	40	30	200
	Hazy Meadow Park Soil	0.160	10	20	40	30	200
	Using T-TDR Sensors						
	ASTM Fine Sand	0	0	20	60	40	400
	ASTM Fine Sand	0.080	5	20	60	40	400
	ASTM Fine Sand	0.160	10	20	60	40	400
	ASTM Fine Sand	0.240	15	20	60	40	400
	ASTM Fine Sand	0.288	18	20	60	40	400

3.7 Analysis of One-Dimensional Heat Transfer

Previous researches determined that one-dimensional heat transfer is reflected by a linear temperature profile in dry soil between two regions of different temperature boundary conditions. As for moist soil, a concave upward temperature profile would indicate non-uniformity of the thermal properties of the soil, when the one-dimensional heat transfer is achieved. In this study, the temperature variations at different locations for both dry and moist soil were assessed to determine whether the one-dimensional conduction was satisfied.

3.8 Analysis of Coupled Thermo-Hydro Behavior of Unsaturated Soil

ASTM fine sand and Hazy Meadow Park soil, mixed with different amounts of water, were compacted in the modified soil cell, and the top and bottom of the cell were subjected to different temperature boundary conditions to create thermal gradients. The migration of water caused by the temperature gradient was then evaluated. Previous researchers have determined that pore water moves from a warm region to a cooler region when thermal gradients come into play. This study will assess, confirm, or contribute to the advancement of the understanding of coupled migration of water and heat in unsaturated soil.

3.9 References

Heitman, J. L., Horton, R., Ren, T. and Ochsner T. E. (2007). "An Improved Approach for Measurement of Coupled Heat and Water Transfer in Soil Cells." Soil Science Society of America Journal 71 (3): 872. https://doi.org/10.2136/sssaj2006.0327.

Lei, G., Kaneza, N., Yu, X., Li, T., Habibzadeh-Bigdarvish, O. (2019). "Development of a One-dimensional Heating Soil Test Cell" ASCE Geo-Congress 2019, Philadelphia, Pennsylvania.

Lei, G., Kaneza, N., Li, T., Habibzadeh-Bigdarvish, O., Yu, X. (2019). “Development and Validation of a Double-Column Soil Cell for 1-D Heating Test” ASCE Geo-Congress 2019, Philadelphia, Pennsylvania.

Prunty, L. and Horton, R. (1994). “Steady-state temperature distribution in non-isothermal, unsaturated closed soil cells.” Soil Sci. Soc. Am. J. 58:1358-1363.

Zhou, J., Heitman, J. L., Horton, R., Ren, T., Ochsner, T. E., Prunty, L., Ewing, R. P., and Sauer, T. J. (2006). “Method for Maintaining One-Dimensional Temperature Gradients in Unsaturated, Closed Soil Cells.” Soil Science Society of America Journal 70 (4): 1303. https://doi.org/10.2136/sssaj2005.0336n.

CHAPTER IV

RESULTS AND DISCUSSIONS

4.1 Introduction

The analysis of the TDR waveforms produced uncalibrated values of K_a and EC_b, and, using the methods described in the Fabrication and Calibration of Sensors section, calibrated values were obtained. The volumetric water content (θ) and gravimetric water content (ω) were determined from the calibrated values of K_a and EC_b and using the equations described below.

- **Gravimetric Water Content** (Topp's Equation)

$$\theta = 4.3\ x\ 10^{-6}Ka^3 - 5.5\ x\ 10^{-4}Ka^2 + 2.92\ x\ 10^{-2}Ka + 5.3\ x\ 10^{-2} \quad (4\text{-}1)$$

$$\omega = \theta \frac{\rho_\omega}{\rho_d} \quad (4\text{-}2)$$

θ = volumetric water content (cm^3/cm^3)

K_a = apparent dielectric constant (-)

ω = gravimetric water content (-)

ρ_ω = density of water (kg/m^3)

ρ_d = dry density (kg/m^3)

- **Gravimetric Water Content** (One-Step Method and a and b Method)

$$\omega = \frac{c\sqrt{Ka} - a\sqrt{ECb}}{b\sqrt{ECb} - d\sqrt{Ka}} \quad (4\text{-}3)$$

$$\omega = \frac{1}{b}\left(\frac{\sqrt{Ka}\,\rho\omega}{\rho d} - a\right) \quad (4\text{-}4)$$

ω = gravimetric water content (-)

K_a = apparent dielectric constant (-)

EC_b = bulk Electrical Conductivity (Sm^{-1})

ρ_ω = density of water (g/cm^3)

ρ_d = dry density (g/cm^3)

a, b, c, d = four specific calibration constants (-)

The calibration constants a, b, c, and d were obtained from the calibration analysis of TDR sensors where the relationship between K_a and oven-dried ω values, as wells as EC_b and oven-dried ω values were established. a is the constant and b the slope of the calibration equation of K_a and ω; whereas, c is the constant and d the slope of the calibration equation of EC_b and ω. The determination of the calibration constants is shown in Figures 19 through 22 and Table 9 and 10. The steps of the calibration analysis went as follows:

- Prepare approximately 1500 g of oven-dried soil.
- Add water to obtain the targeted water content. Mix the soil and water thoroughly.
- Weigh empty mold without its collar. Attach the collar on the empty mold.
- Fill mold with about 420 g of the soil and compact it using a rammer. Repeat this step twice for a total of three (3) evenly compacted layers.
- After compaction, remove the collar and use a straight edge to scrape the excess soil.
- Weigh the mold with the compacted soil.
- Place a small plastic wrap on top of the mold so as not to let the water evaporate. Re-attach the collar on the mold and place the latter horizontally.
- Insert each TDR sensor into the soil of the corresponding Proctor mold and start collecting TDR waveforms of K_a and EC_b, using the PC200W software. Connect the TDR sensors to a multiplexer then connect the multiplexer to the TDR100 for data collection.
- Weight empty cans for moisture content determination.
- Collect two (2) samples of the soil surrounding the location of the sensors and pour into

the empty cans. Place the cans into the oven for 24 hours.

- Weigh the oven-dried samples. Determine the ω and repeat all steps for another sample.

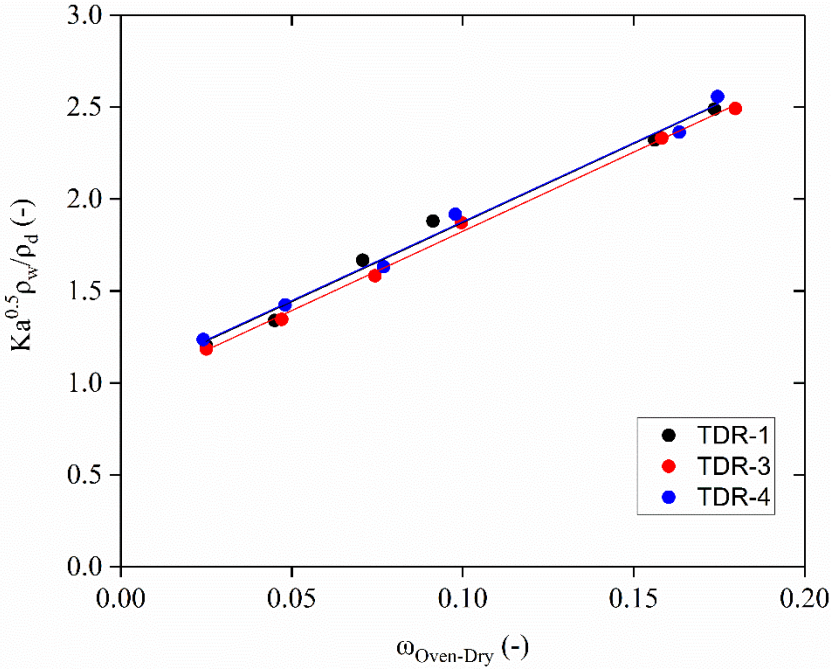

Figure 19. Determination of constants a and b for ASTM fine sand.

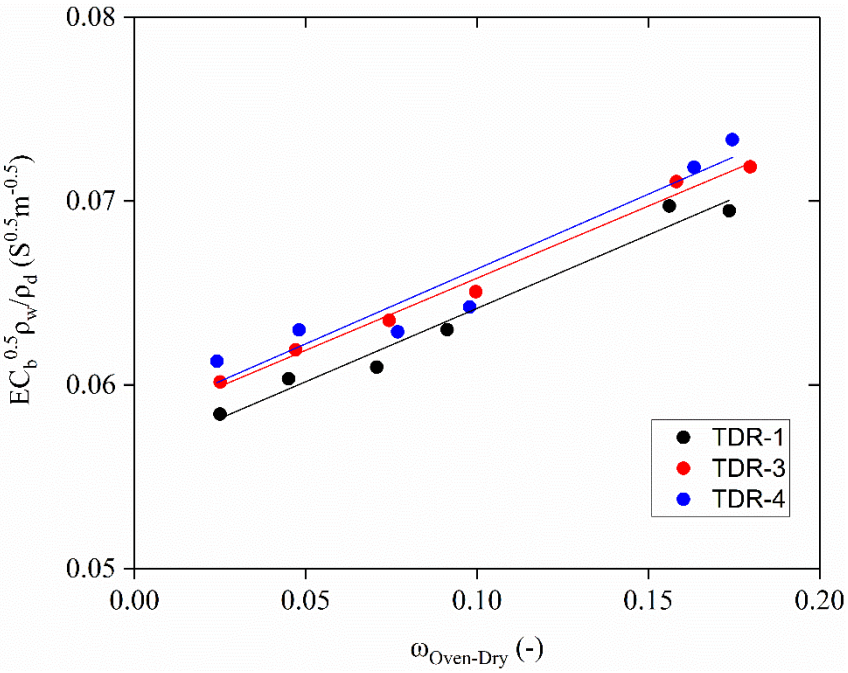

Figure 20. Determination of constants c and d for ASTM fine sand.

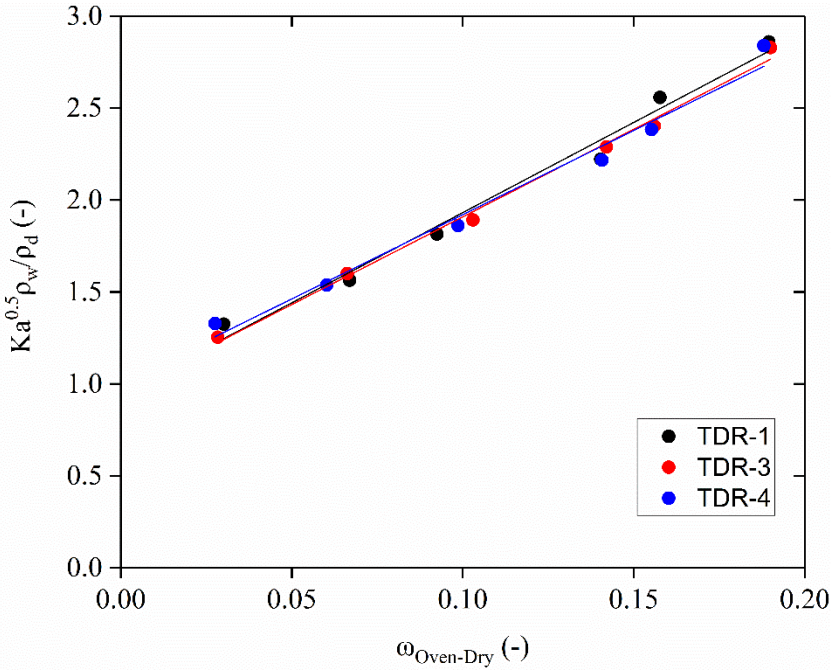

Figure 21. Determination of constants a and b for Hazy Meadow Park soil.

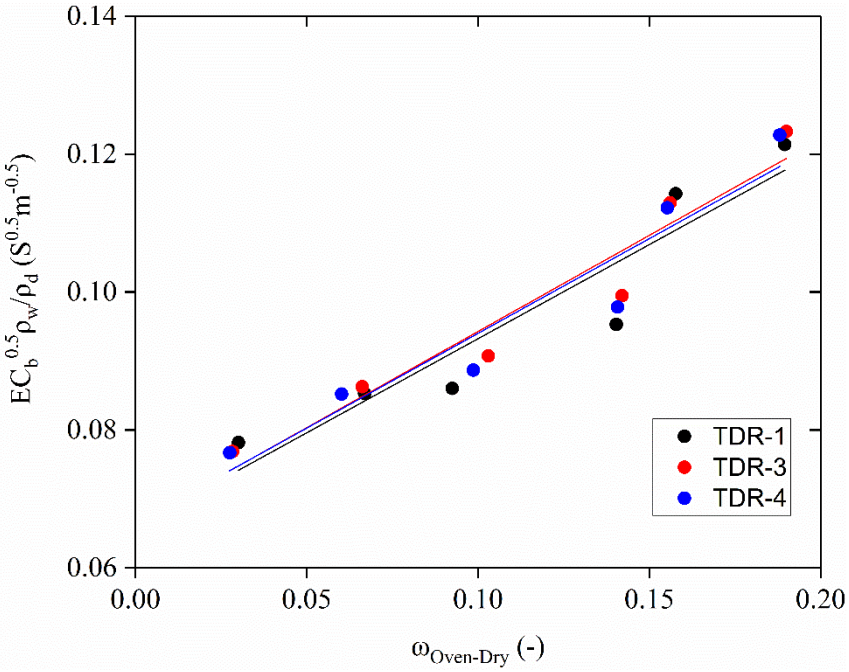

Figure 22. Determination of constants c and d for Hazy Meadow Park soil.

Table 9. Determination of One Step Method calibration constants for ASTM fine sand.

Sensors	a	b	c	d
TDR-1	1.0124	8.5905	0.0562	0.0798
TDR-3	0.9624	8.6166	0.0580	0.0784
TDR-4	1.0187	8.5777	0.0582	0.0814

Table 10. Determination of One Step Method calibration constants for Hazy Meadow Park soil.

Sensors	a	b	c	d
TDR-1	0.9507	9.8050	0.0659	0.2729
TDR-3	0.9550	9.5297	0.0664	0.2789
TDR-4	1.0041	9.1604	0.0665	0.2748

The calibration constants established from the calibration analysis were used to determine ω using the One Step Method. These results were compared with the ω measured by the oven-drying method, in addition to the values calculated by the Topp's equation. This comparison is illustrated graphically in Figures 23 through 28. Predominantly, the ω values calculated by the Topp's equation do not deviate from the oven-dried ω for more than 0.01 (1% of moisture), expect for higher values of ω. This is also the case for the values obtained by the One Step Method; however, the ω values corresponding to the oven-dried ω of about 14% appear to deviate significantly for all the TDR sensors, especially considering the Hazy Meadow Park soil. Overall, the performance of the TDR sensors was satisfactory.

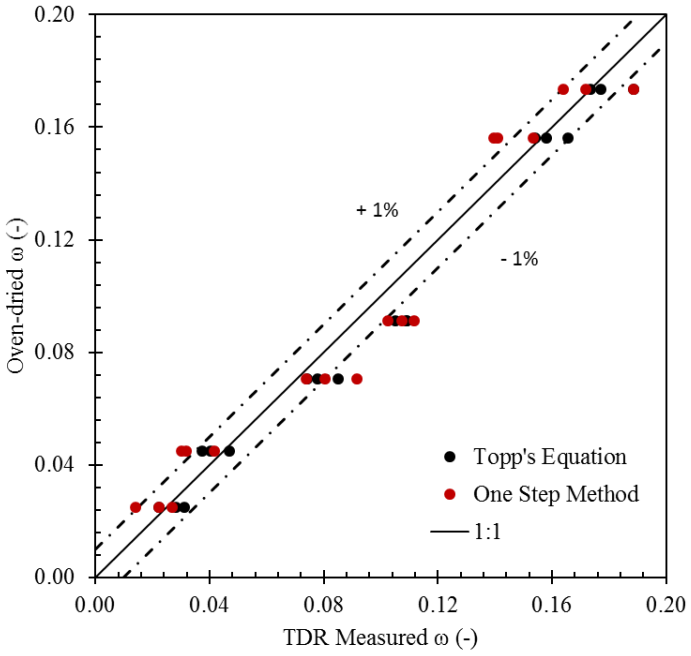

Figure 23. TDR-1 calibration analysis for ASTM fine sand.

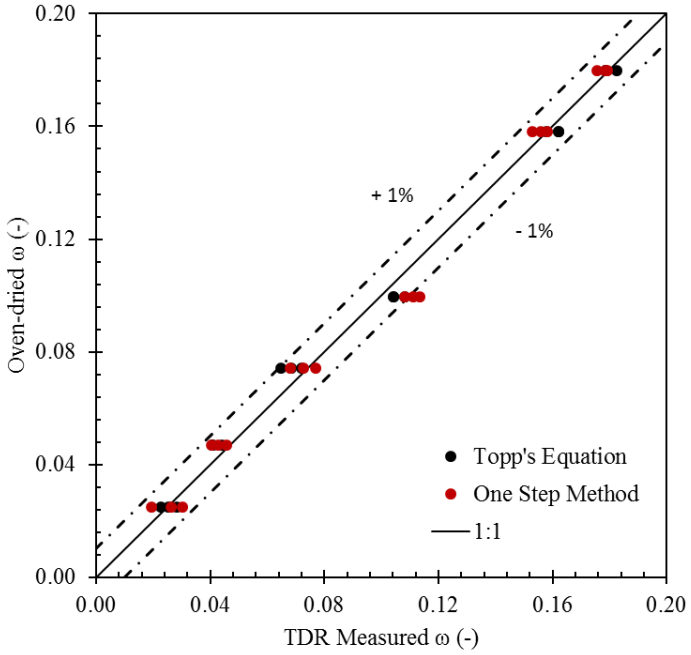

Figure 24. TDR-3 calibration analysis for ASTM fine sand.

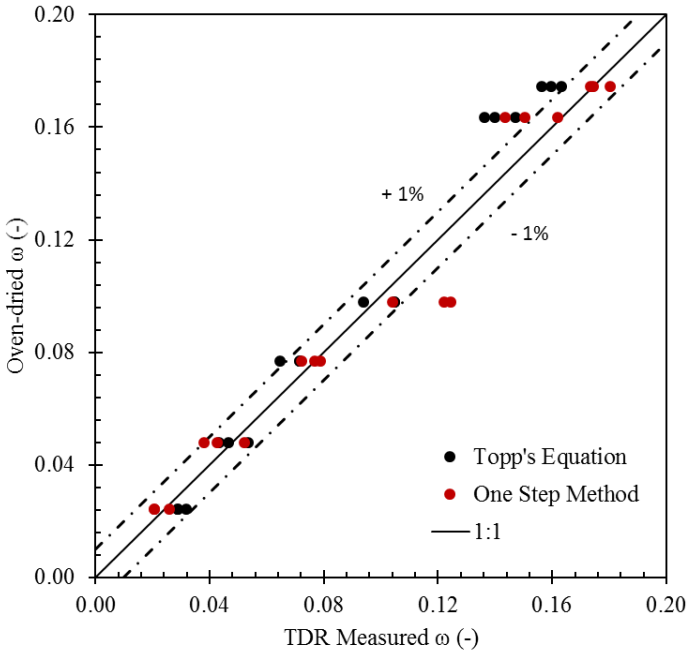

Figure 25. TDR-4 calibration analysis for ASTM fine sand.

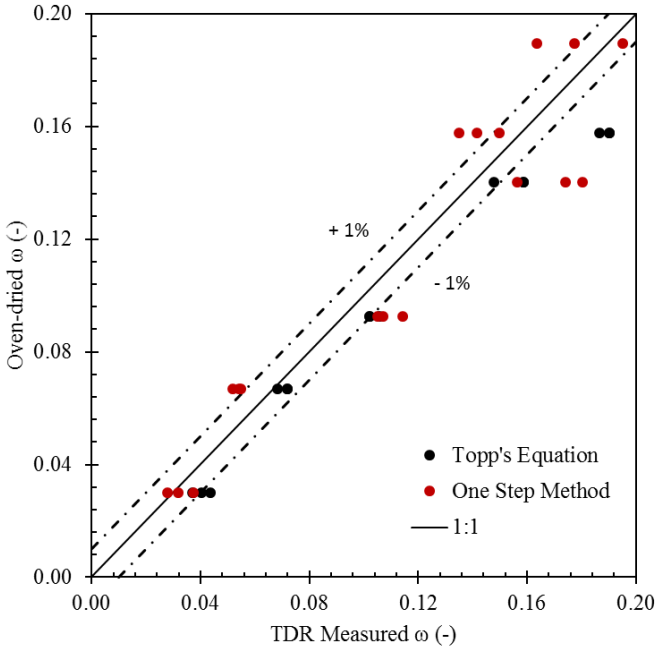

Figure 26. TDR-1 calibration analysis for Hazy Meadow Park soil.

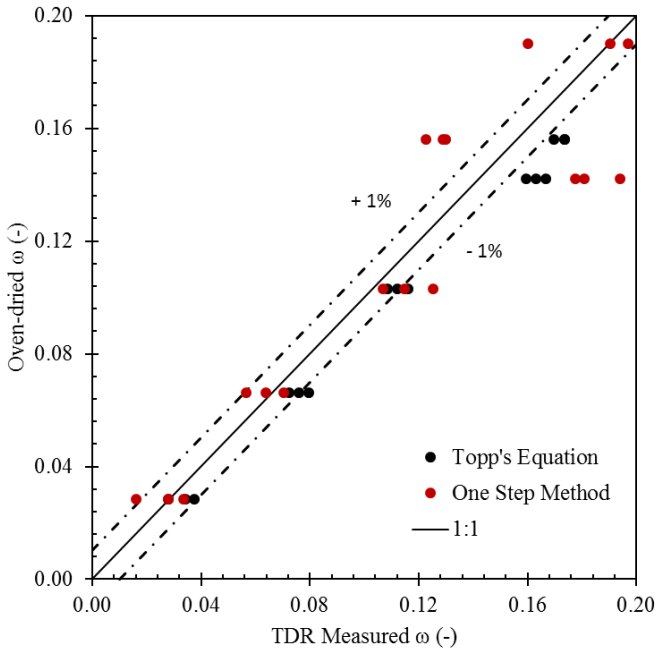

Figure 27. TDR-3 calibration analysis for Hazy Meadow Park soil.

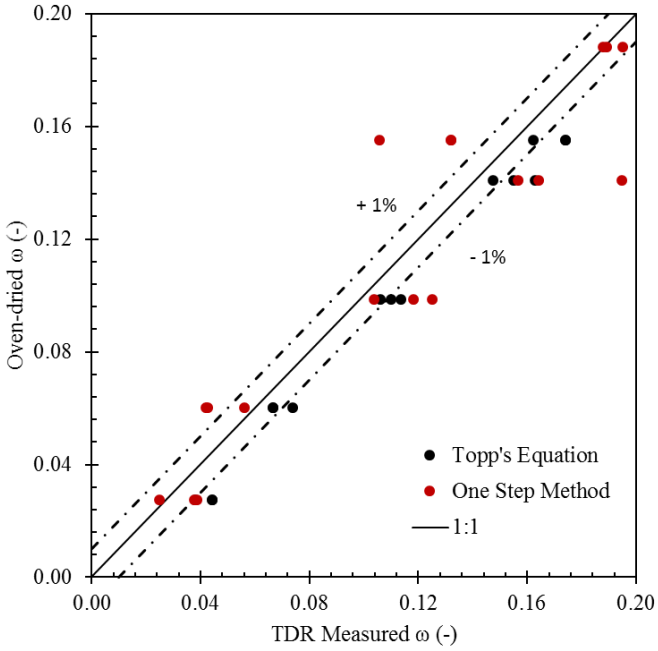

Figure 28. TDR-4 calibration analysis for Hazy Meadow Park soil.

4.2 Maintaining One-Dimensional Heat Transfer

Preliminary heating tests were carried out to analyze one-dimensional heat transfer inside the modified soil cell. ASTM fine sand and Hazy Meadow Park soil were tested for a moisture content of approximately 0%. Dry sand was placed in the modified soil cell using a funnel. The heat exchangers were then subjected to temperature boundaries of 60°C (ASTM fine sand) and 40°C (Hazy Meadow Park soil) for the lower exchanger and 20°C for the upper exchanger after the soil had reached approximately 23°C of initial temperature. The temperature distribution inside the cell is illustrated in Figures 29 and 32. The heating lasted about 2 days. Around 4 hours after setting the boundary temperatures, steady-state temperatures were reached.

In Figures 30 and 34, the dots indicate the temperature distribution at steady-state and the dotted lines indicate the theoretical one-dimensional heat conduction in dry soil. A clear linear trend of the temperature variation is observed in the soil cell. At the middle of the cell, however, the temperature of the soil deviates from the linear trend. This observation suggests that the ambient temperature may have interfered with the temperature of the soil specimens, which resulted in a concave upward temperature profile, instead of a linear profile. The reason behind this is that no insulation was applied to the modified soil cell. Another test was performed (Figure 35), where the dry ASTM fine sand was heated and approximately 8.9 cm (3.5 in.) fiberglass insulation from Owens Corning was installed to limit the interference of the ambient temperature with that within the soil testing cell. Based on these results, the modified soil cell was considered to have a feasibility of maintaining one-dimensional heat transfer if adequate insulation is applied. During the study of one-dimensional heat transfer, the thermal properties of dry ASTM fine sand and Hazy Meadow Park soil were also determined (Figures 31 and 33).

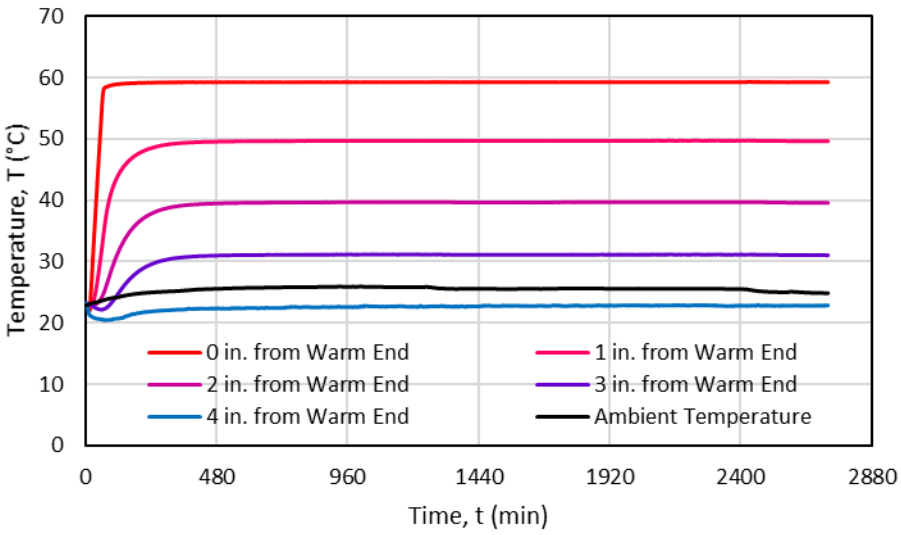

Figure 29. Temperature variations for ASTM fine sand (target ω = 0%).

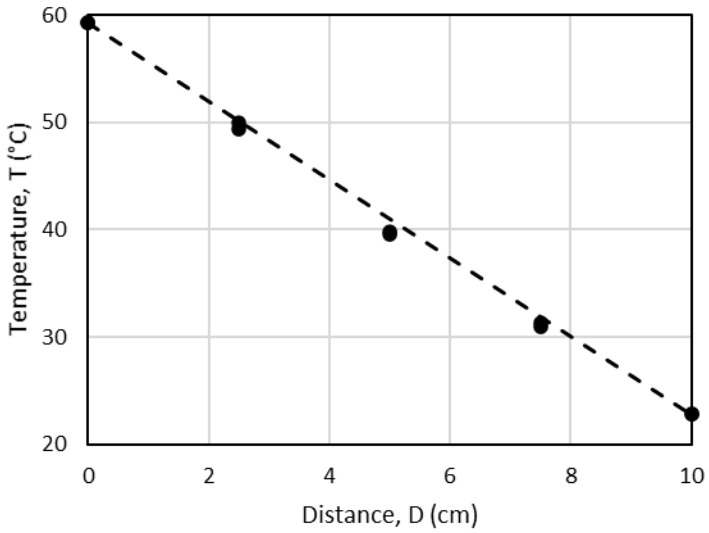

Figure 30. Steady-state temperature distributions of ASTM fine sand; ω = 0%.

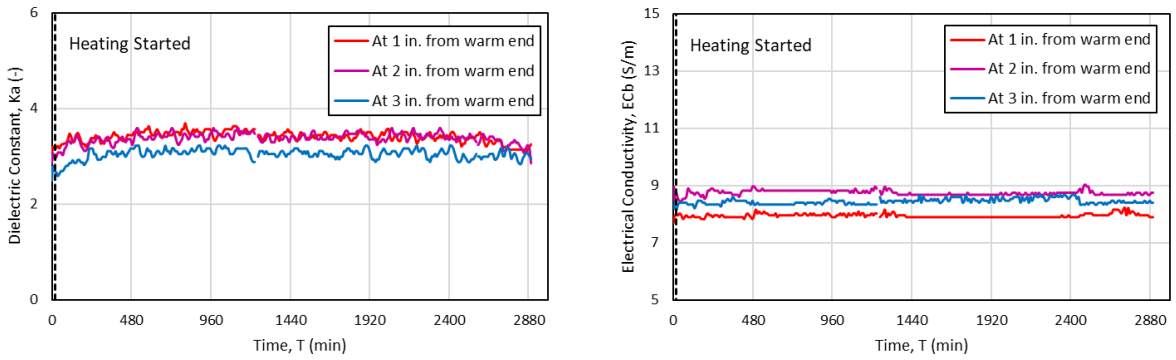

Figure 31. K_a and EC_b of ASTM fine sand; ω = 0%.

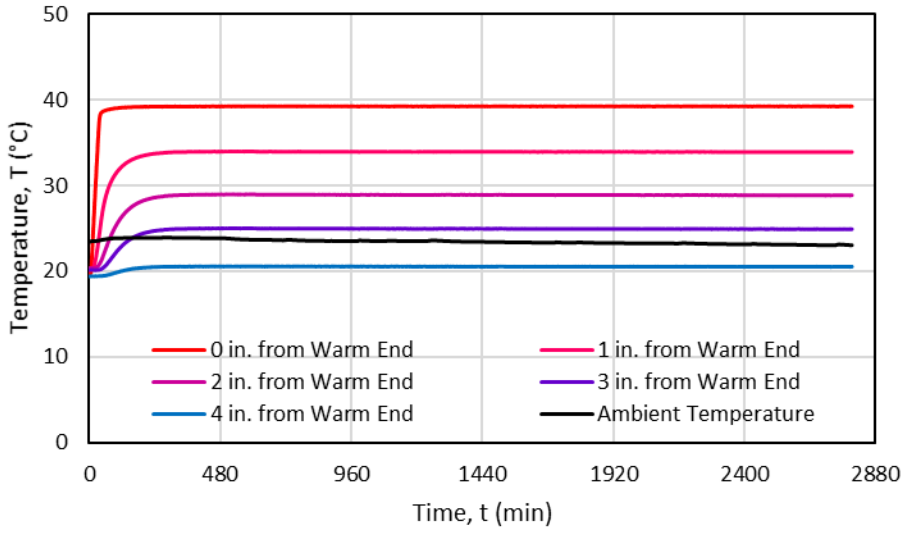

Figure 32. Temperature variations for Hazy Meadow Park soil (target ω = 0%).

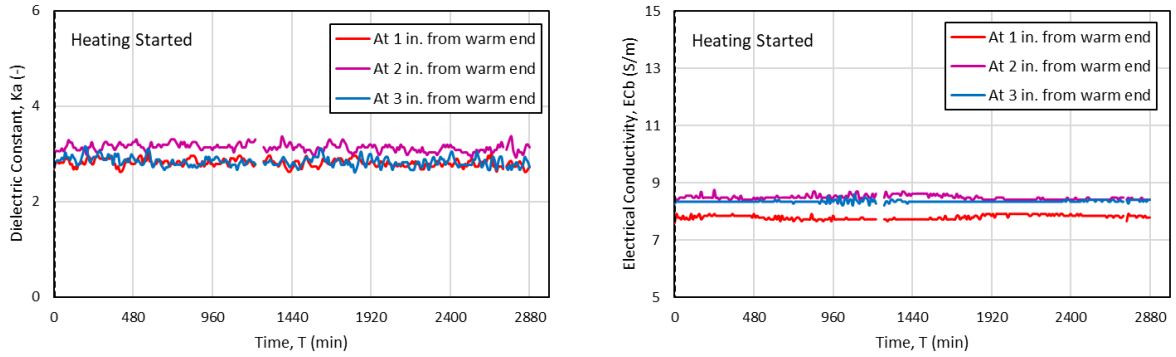

Figure 33. K_a and EC_b of Hazy Meadow Park soil; ω = 0%.

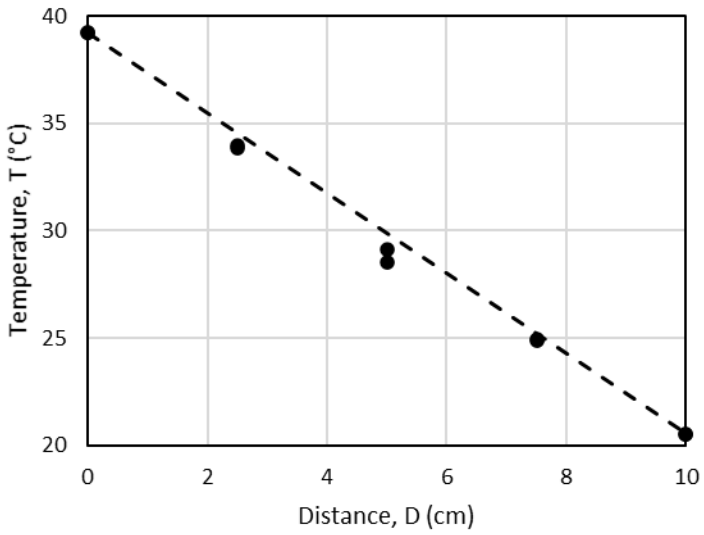

Figure 34. Steady-state temperature distributions of Hazy Meadow Park soil; ω = 0%.

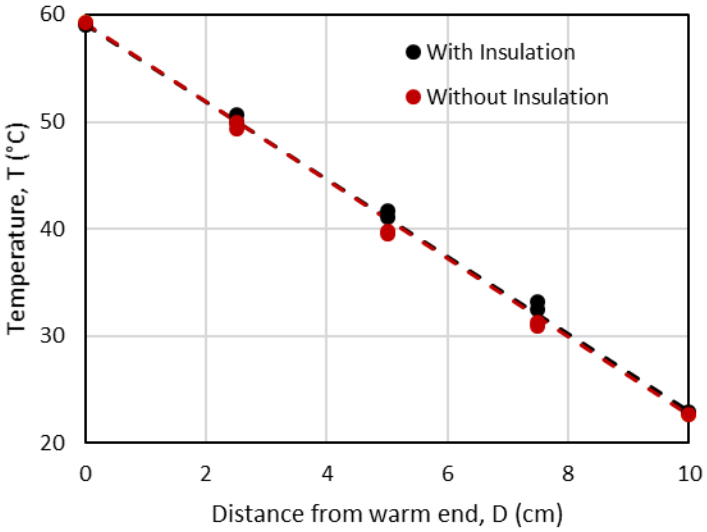

Figure 35. Steady-state temperature distributions of ASTM fine sand, with insulation; ω = 0%.

4.3 Coupled Thermo-Hydro Behavior of Unsaturated Soil

The temperature variations right before, during, and after imposing boundary temperature on the upper and lower heat exchangers are illustrated in Figures 36, 38, 40 and 42. In addition, steady-state temperatures (from the warm end to the cool end) representing the last 60 min of the

96 hr heating period are shown in Figure 37, 39, 41, and 43. In the latter figures, the dots, indicating steady-state temperatures, show non-linearity with respect to the dotted lines that delineate linearity, and this observation confirms the non-uniformity of thermal properties of ASTM fine sand and Hazy Meadow Park soil that result from a non-uniformity of thermal properties of unsaturated soil under non-isothermal conditions. These solid lines show a concave downward temperature profile, which indicate the presence of ambient temperature interference (Prunty and Horton, 1994). The concave temperature profile is more evident for ASTM fine sand than it is for Hazy Meadow Park soil and is more apparent for the ASTM fine sand with a higher moisture content. This may suggest that the temperature profile shape has a correlation with the thermal gradient magnitude or air voids volume, since the Hazy Meadow Park soil has more fine particles than ASTM fine sand.

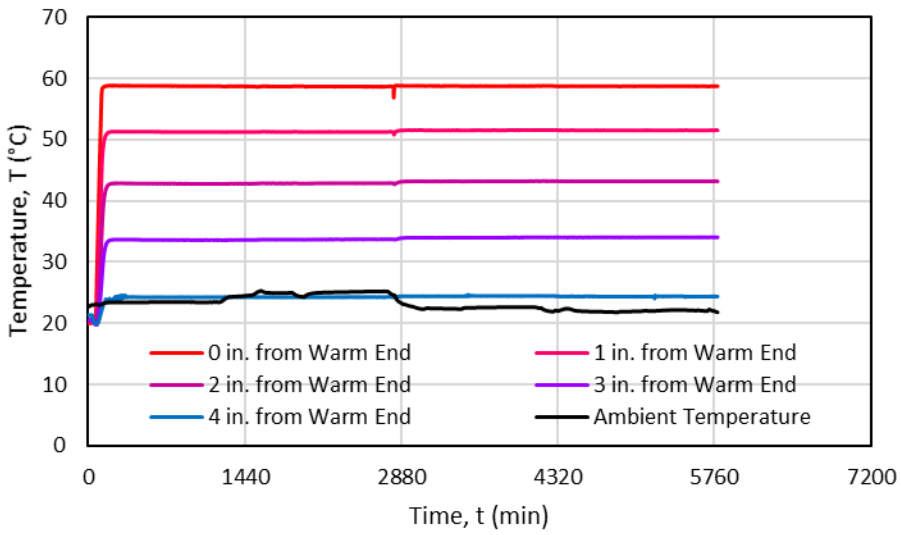

Figure 36. Temperature variations for ASTM fine sand (target ω = 6%).

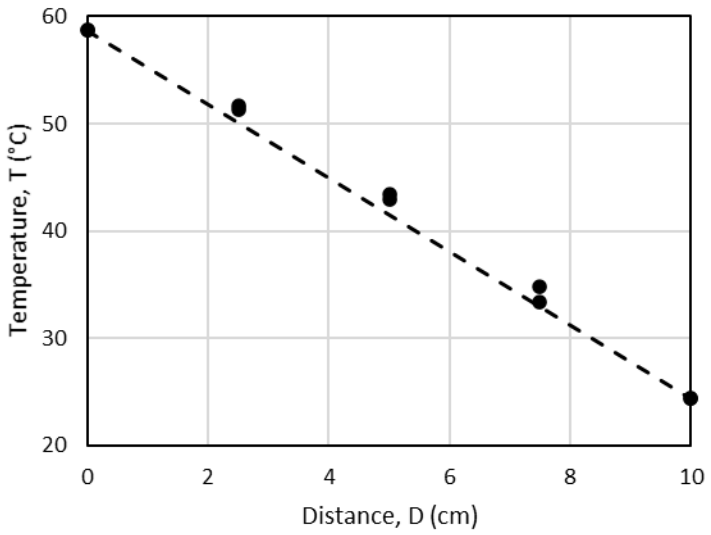

Figure 37. Steady-state temperature distributions of ASTM fine sand (target ω = 6%).

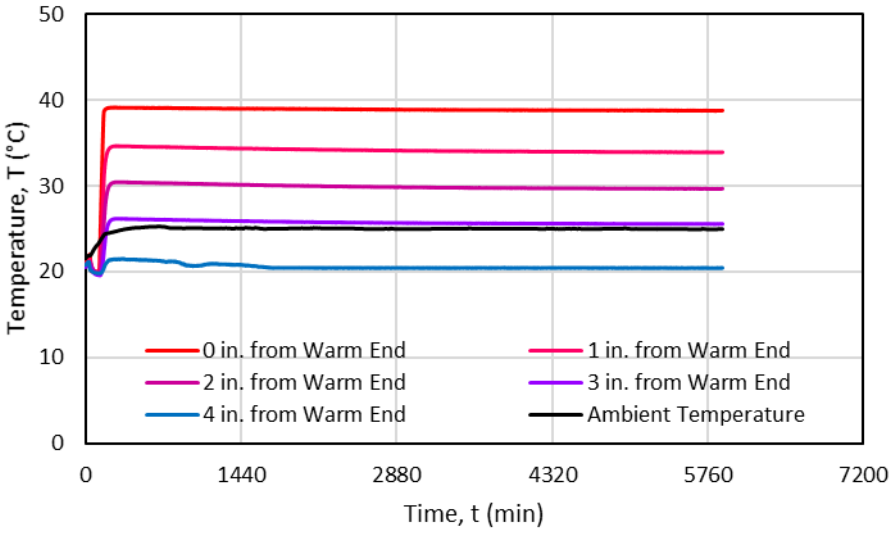

Figure 38. Temperature variations for Hazy Meadow Park soil (target ω = 6%).

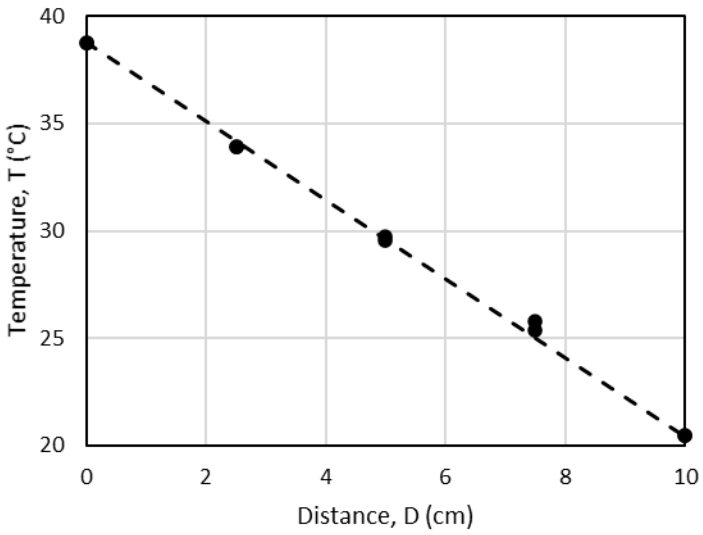

Figure 39. Steady-state temperature distributions of Hazy Meadow Park soil (target ω = 6%).

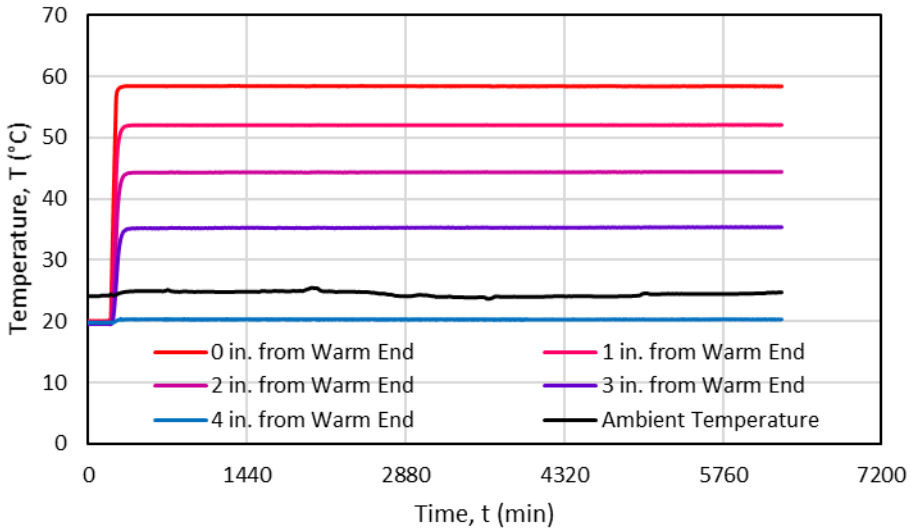

Figure 40. Temperature variations for ASTM fine sand (target ω = 10%).

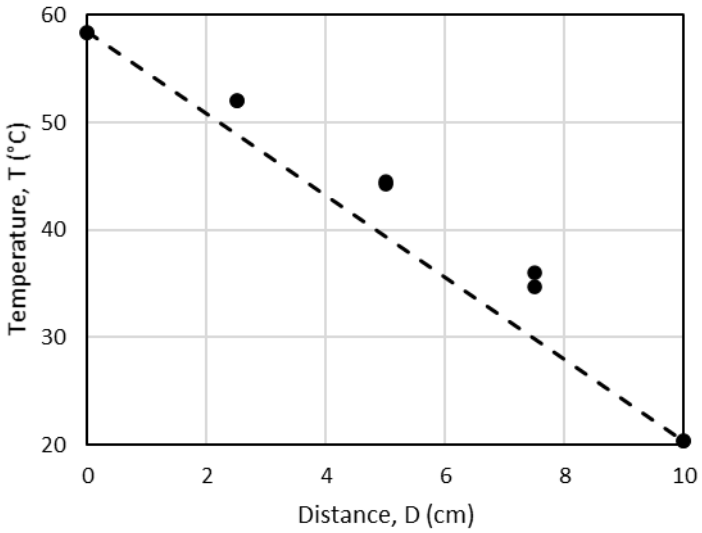

Figure 41. Steady-state temperature distributions of ASTM fine sand (target ω = 10%).

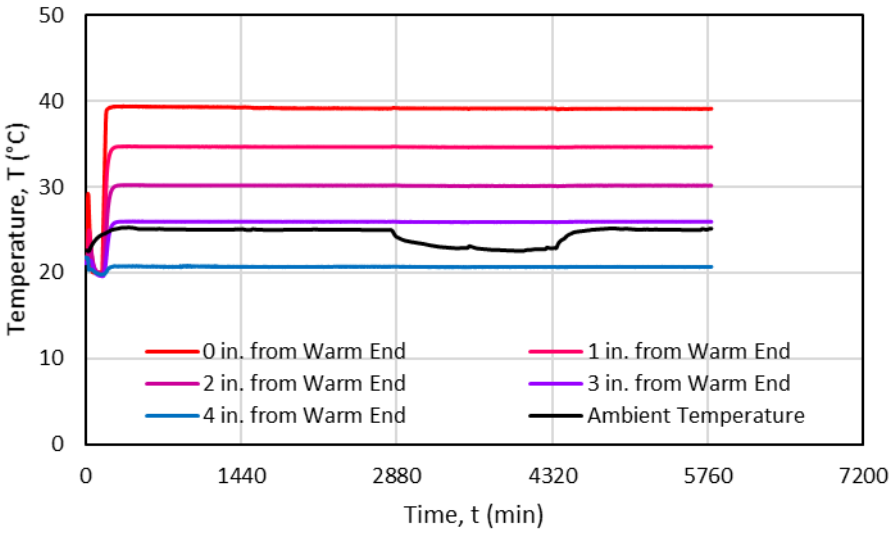

Figure 42. Temperature variations for Hazy Meadow Park soil (target ω = 10%).

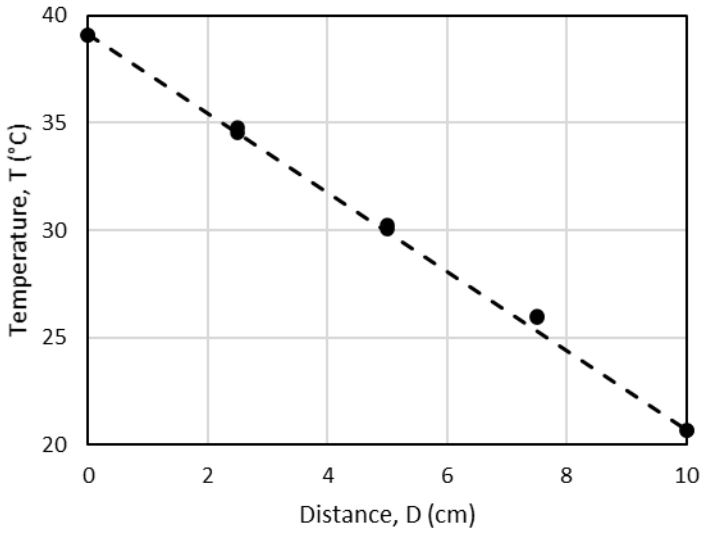

Figure 43. Steady-state temperature distributions of Hazy Meadow Park (target ω = 10%).

Following the analysis of the temperature distributions, the moisture content of the ASTM fine sand and Hazy Meadow Park soil was evaluated. The waveforms of the K_a and EC_b were measured by the TDR100 moisture meter to determine the water content of the two soil samples. The variations of these two properties are depicted in Figures 44 through 47.

The K_a of ASTM fine sand for target ω of 6 and 10% show a relatively similar trend. In both cases, the K_a values of the soil located at 2.5 cm from the warm end are higher than those of the soil at 5.0 and 7.5 cm. Since K_a is directly proportional to ω, this means that more water has been retained at the bottom of the cell. This is reasonable, because ASTM fine sand is a poorly graded soil, thus is rather particularly porous, and, when mixed with water, the pore water tends to drop down, due to gravity. Conversely, the Hazy Meadow Park soil contains grains of smaller sizes and is less likely to have pore water settle at the bottom of the cell. Therefore, the K_a values of the soil at the three locations of the Hazy meadow Park soil sample were close to each other for major part of the experiment. In general, the K_a values did not show any significant change during

the heating process. The EC_b of the two soil samples increased just after temperature boundaries were imposed on the heat exchangers. This increase was more significant at 2.5 cm from the warm end. The EC_b then gradually but slightly decreased.

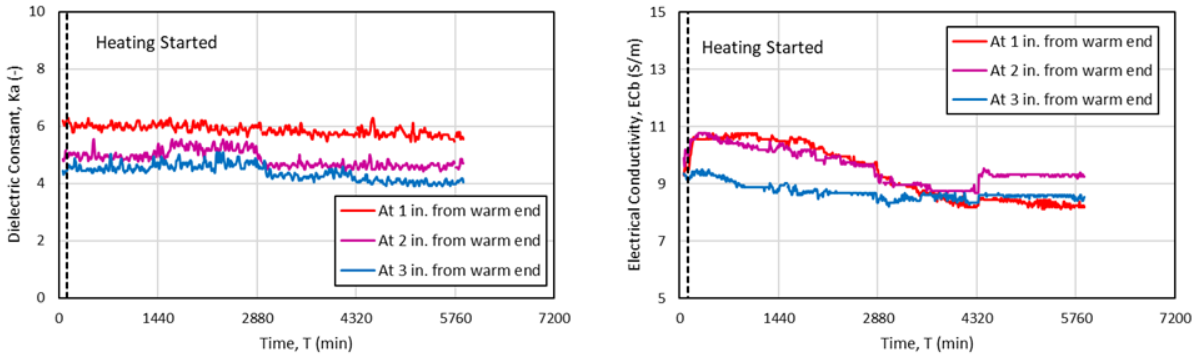

Figure 44. K_a and EC_b of ASTM fine sand; ω = 6%.

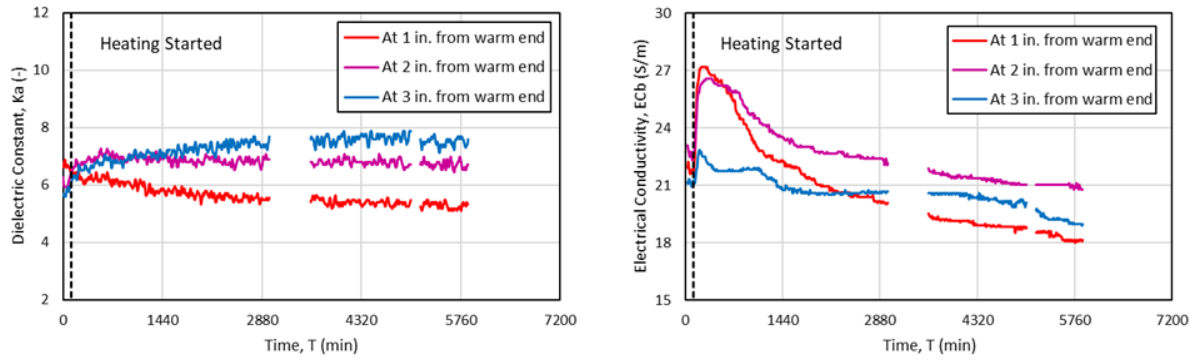

Figure 45. K_a and EC_b of Hazy Meadow Park soil; ω = 6%.

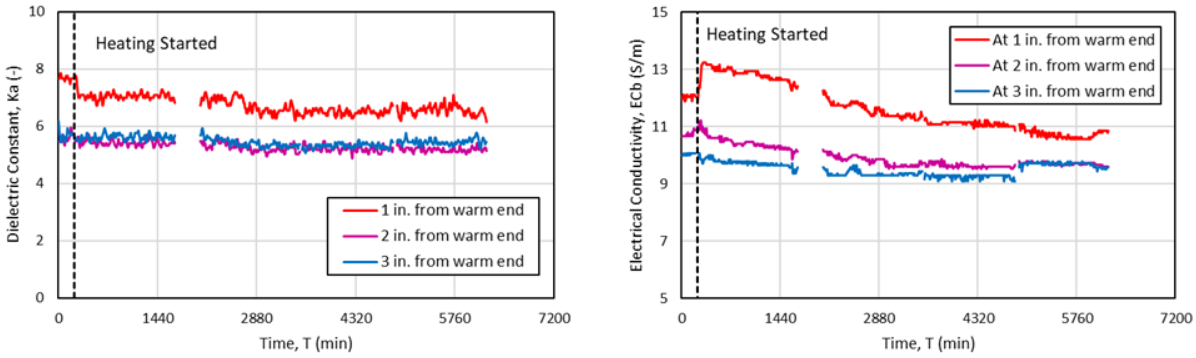

Figure 46. K_a and EC_b of ASTM fine sand; ω = 10%.

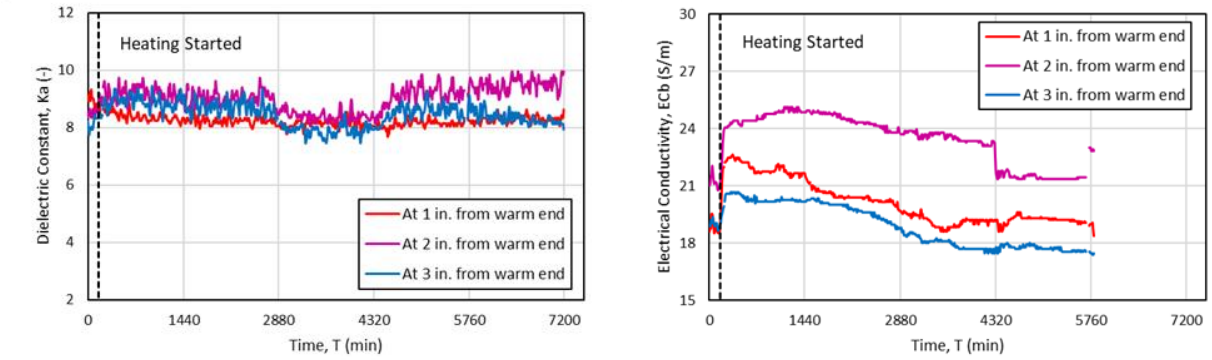

Figure 47. K_a and EC_b of Hazy Meadow Park soil; ω = 10%.

After obtaining the K_a and EC_b values from the methods described above, ω was calculated using Topp's Equation and the One Step Method. Topp's Equation uses only the K_a value to establish the water content, whereas the One Step Method uses both the K_a and EC_b values. The trend of ω obtained using Topp's equation is similar to that of K_a, since the two are directly proportional. As for the ω obtained from the One Step Method, it is inversely proportional to the EC_b.

The final and nearly steady-state values of ω calculated using the Topp's Equation follow relatively the same trend for ASTM fine sand and Hazy Meadow Park soil, while the values of One Step Method deviate from the rest. In general, the values obtained using the One Step Method do not conform to any specific pattern. This discrepancy resulted from the values of EC_b: the EC_b may be influenced by other factors other than heat and water movement and that are out of the scope of this study. Consequently, an alternate method was adapted and was called the a and b method. It involved the calibration constants a and b from the One Step method, and it was used to calculate the ω. The obtained ω values from the two methods, presented in Figures 48 through 55, were compared with the ω obtained from the oven-drying method. The figures below show that the values of ω obtained from the oven-drying method are close to those obtained from the

two methods at nearly steady-state. Figure 53 does not include the measurement of the oven-dried ω, because soil samples were not collected at the end of the test for ω determination when running the test of ASTM fine sand for a target ω of 10%.

The initial values of ω (the ω calculated from the samples collected during the packing) are also portrayed in Figures 49, 51, 53, and 55. The graphs indicate that there has been a certain loss and even a certain gain, perhaps due to the evaporation of water and resulting from the migration of moisture. The average changes in moisture content is 0.99% for ASTM fine graded sand and 0.74 (target ω = 6%) and 0.32% (target ω = 10%) for Hazy Meadow Park soil.

Many researchers (Bouyoucous, 1915; Jackson et al., 1973; Cahill and Parlange 1998; Heitman, 2007) have established the coupling of moisture and heat transfer in unsaturated soil. They specified that the relocation of soil moisture occurs when the soil is subjected to thermal gradients and that heat also migrates in response to the moisture migration. Pore water has been determined to move from a warm region to a cooler region.

In this study, it was observed that even if some migration of soil moisture did take place, it was not very obvious, especially for ASTM fine sand. This is due to the consistency of the grain sizes of the ASTM fine sand, which makes is poorly graded and particularly porous and permeable. Considering the 96-hr period of heating, the soil water might have settled down at the bottom of the soil cell over time due to gravity. Instead of migrating from the warm end (bottom of the cell) to the cool end (top of the cell), the soil moisture located in the region of approximately 2.5 cm from the warm end remained in the same place, and some of the water from the cooler regions moved down. The Hazy Meadow Park soil is less porous and less permeable; thus, not much water was retained at the bottom of the cell. The distribution of water in the figures below show that the Hazy Meadow Park soil better displays better a good demonstration of how water moves from a

warm region to a cooler region due to thermal gradients, and this is even clearer in Figures 50 and 51, where the initial ω is lower (target ω = 6%). It was observed that moisture migration did not occur from warm end to cool end for the Hazy Meadow Park soil with the initial moisture content of 10%. This may suggest that 10% is greater than the critical moisture content of the Hazy Meadow Park soil, because when the critical moisture content is reached, the soil hydraulic processes are controlled by the strong attractive forces of soil for water, which makes it difficult for moisture to move, according to Bouyoucous (1915).

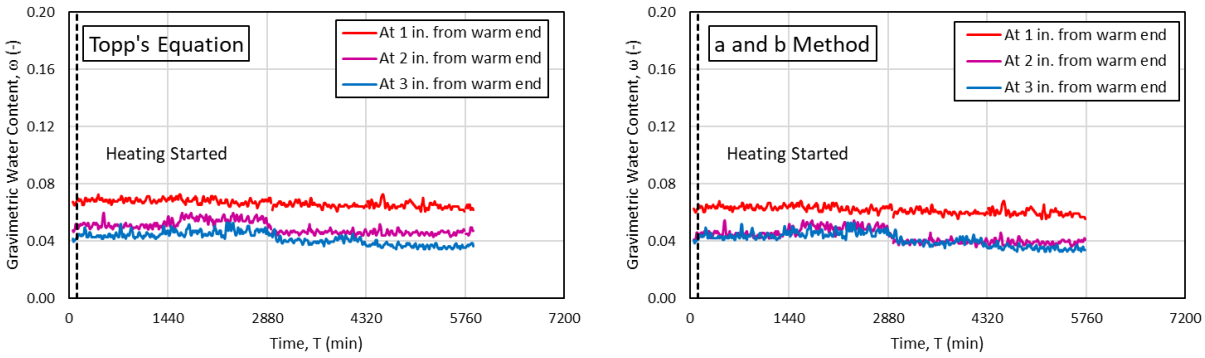

Figure 48. Gravimetric water content of ASTM fine sand (target ω = 6%).

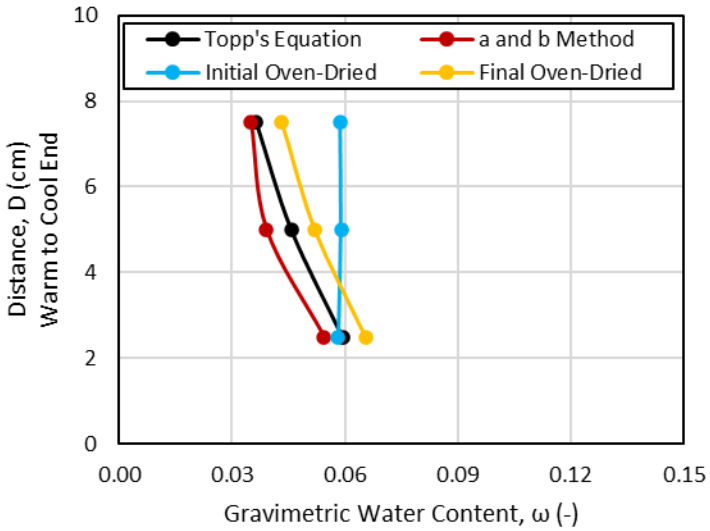

Figure 49. Nearly steady-state moisture distributions of ASTM fine sand (target ω = 6%).

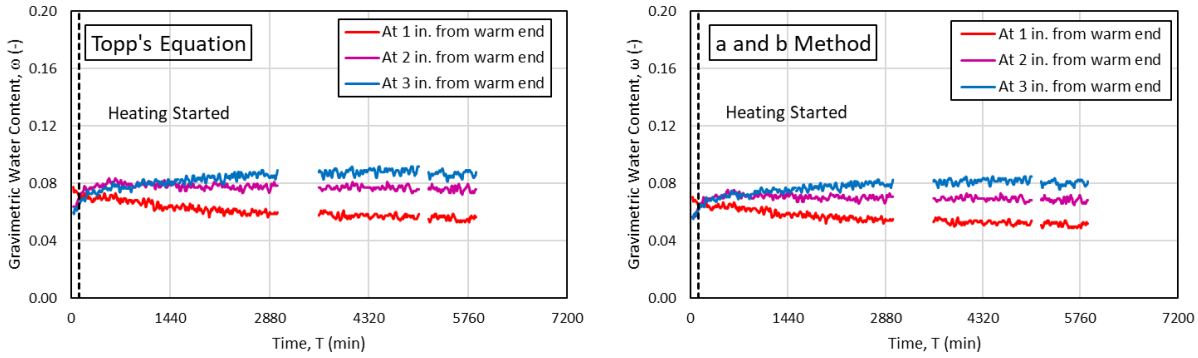

Figure 50. Gravimetric water content of Hazy Meadow Park soil (target ω = 6%).

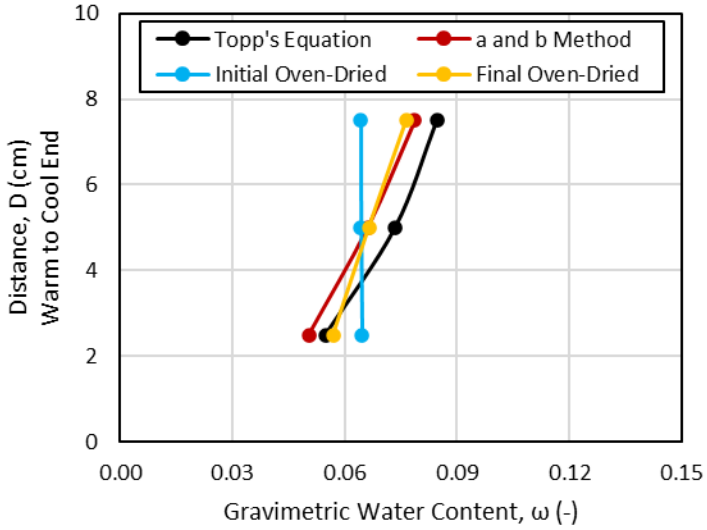

Figure 51. Nearly steady-state moisture distributions of Hazy Meadow Park soil (target ω = 6%).

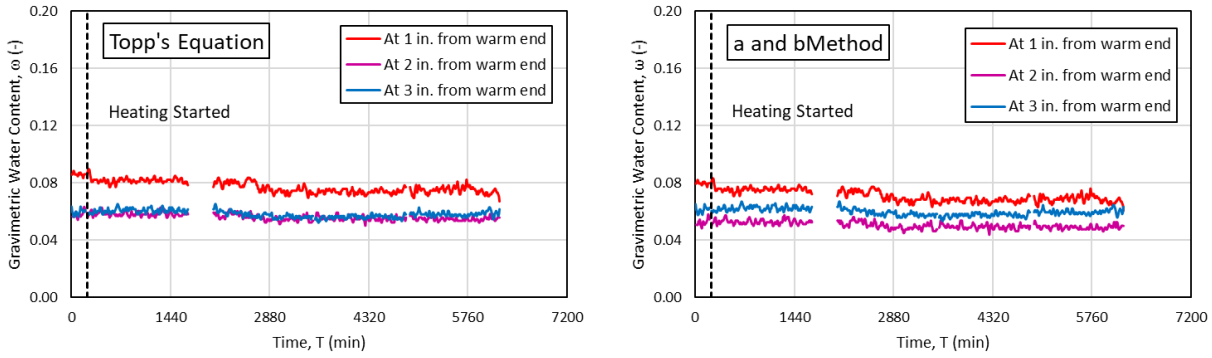

Figure 52. Gravimetric water content of ASTM fine sand (target ω = 10%).

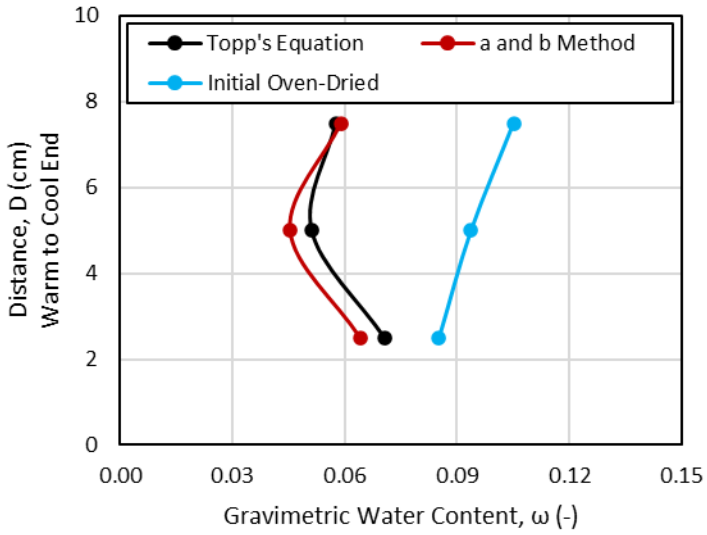

Figure 53. Nearly steady-state moisture distributions of ASTM fine sand (target ω = 10%).

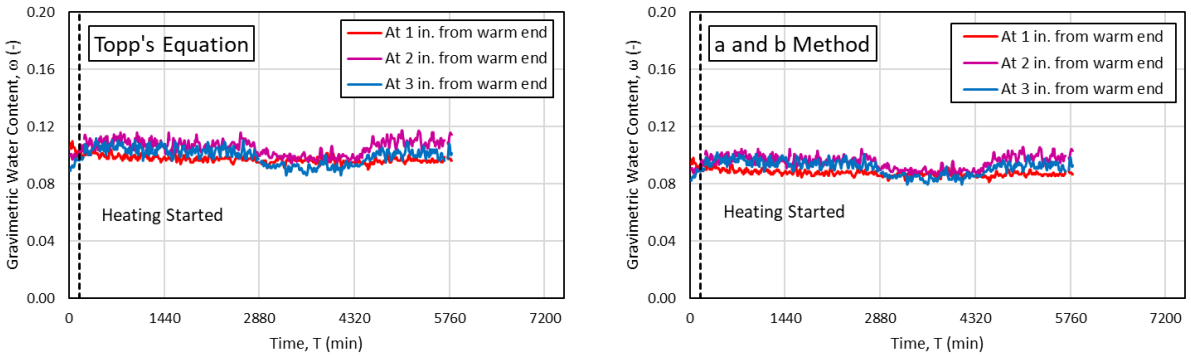

Figure 54. Gravimetric water content of Hazy Meadow Park soil (target ω = 10%).

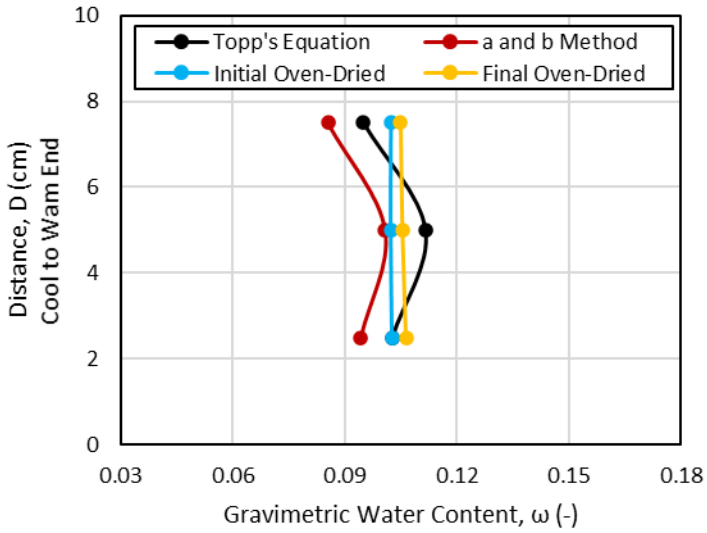

Figure 55. Nearly steady-state moisture distributions of Hazy Meadow Park soil (target ω = 10%).

The following figures, 56 through 63, show the thermos-TDR measured soil moisture distributions when ASTM fine sand was subjected to thermal gradients. The ω was calculated using Topp's equation only, because, during these tests, only the K_a values was measured. There were no significant variations in moisture throughout the heating period other than the first minutes after the start of heating and after several hours of heating (for target ω = 18%). The same behavior of water retention due to porosity and permeability of ASTM fine sand was observed in these tests as in the previous ones. For the lower initial ω (5 and 10%), a large amount was retained in the middle of the cell. Finally, the figures below present the transient and nearly steady-state moisture distributions for ASTM fine sand. They show the calculated values of Topp's equation and the measured oven-dried initial and final values of ω. There was a loss of moisture caused by evaporation during heating. A similar pattern of moisture migration is observed as in the previous tests. Average variations in moisture content are 0.98, 2.23, 2.94, and 4.82% for target moisture contents of 5, 10, 15, and 18%, respectively.

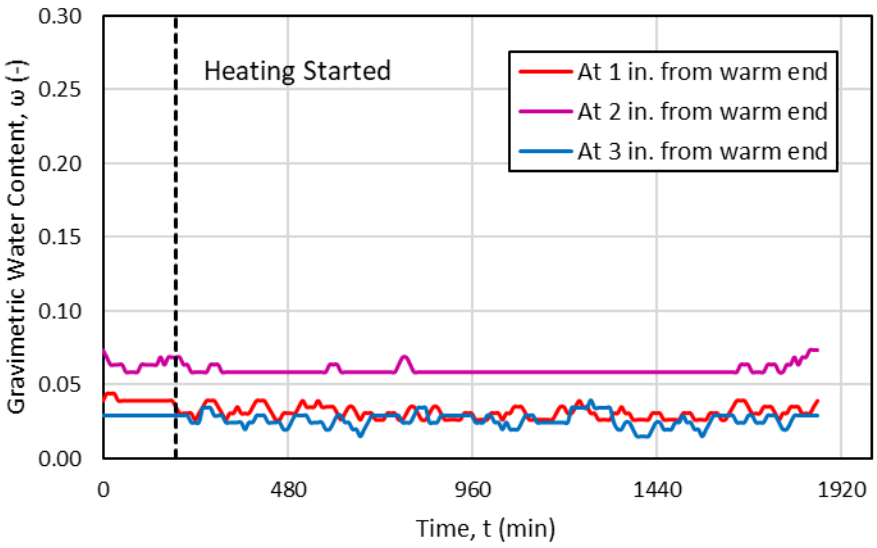

Figure 56. Gravimetric water content of ASTM fine sand (target ω = 5%).

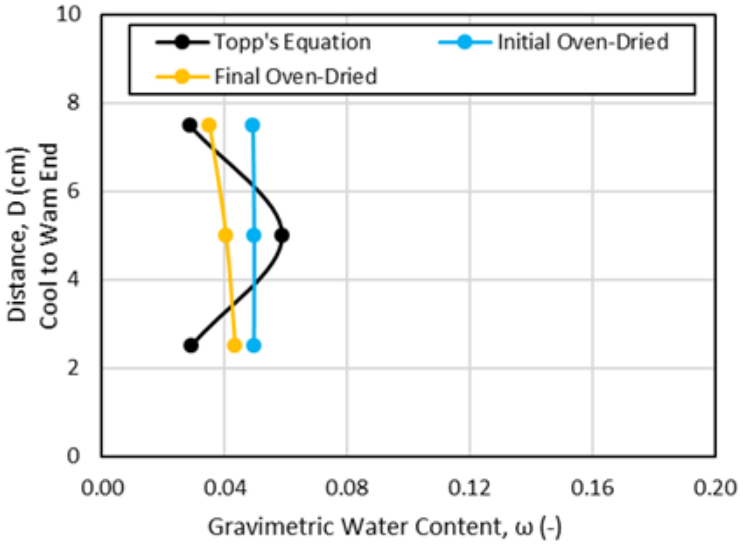

Figure 57. Transient moisture distributions of ASTM fine sand (target ω = 5%).

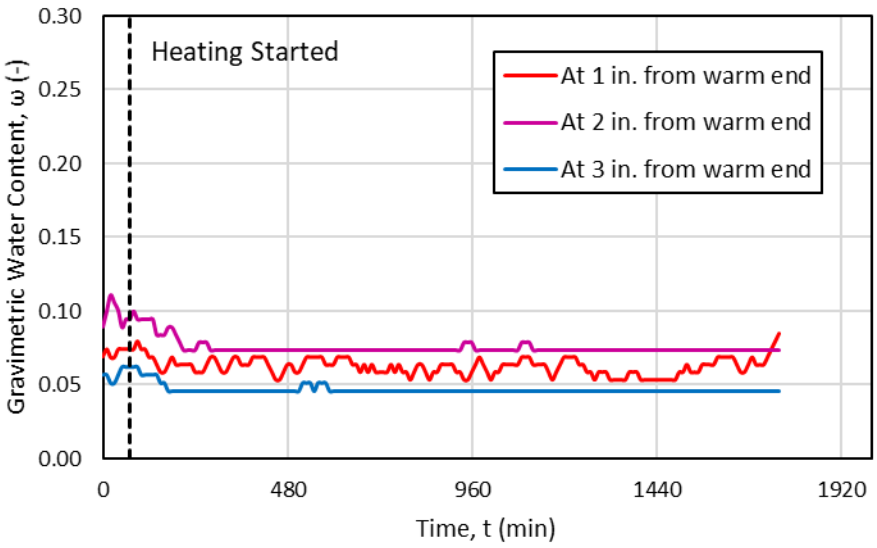

Figure 58. Gravimetric water content of ASTM fine sand (target ω = 10%).

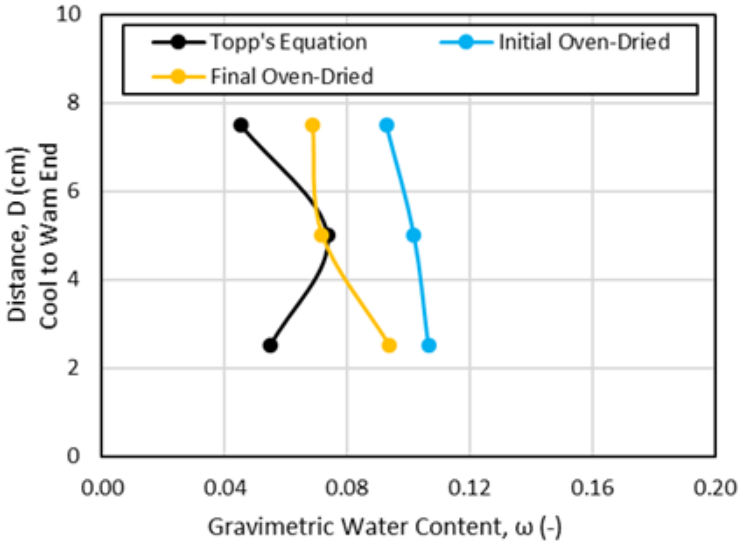

Figure 59. Transient moisture distributions of ASTM fine sand (target ω = 10%).

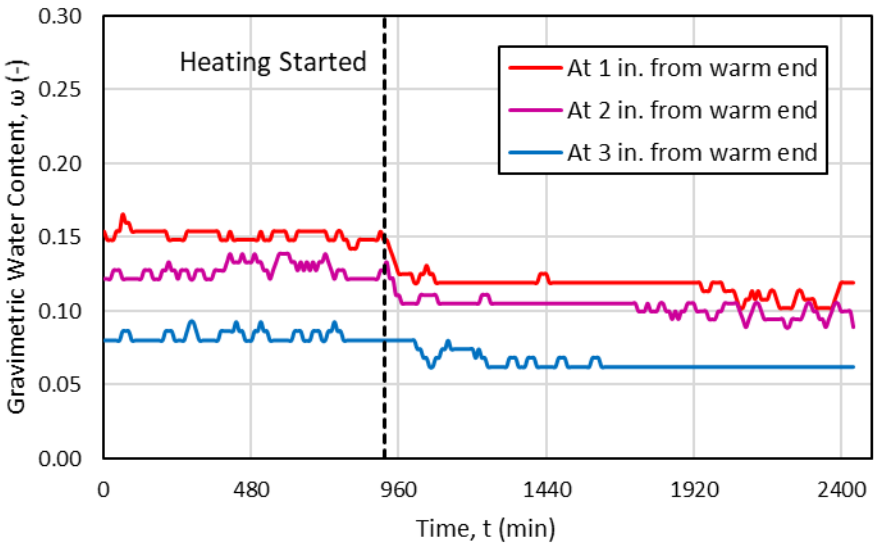

Figure 60. Gravimetric water content of ASTM fine sand (target ω = 15%).

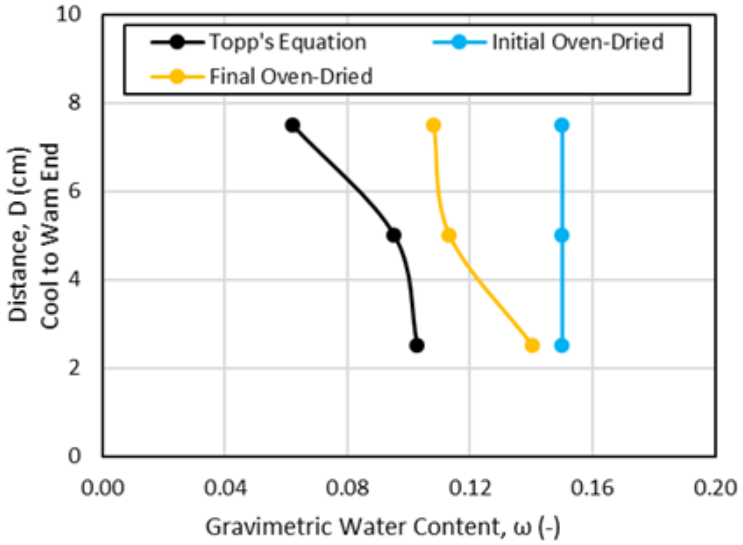

Figure 61. Transient moisture distributions of ASTM fine sand (target ω = 15%).

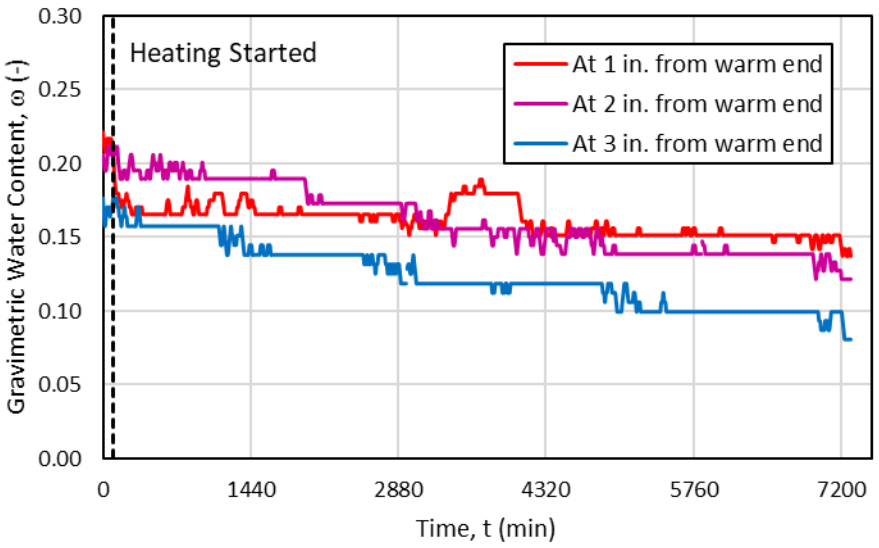

Figure 62. Gravimetric water content of ASTM fine sand (target ω = 18%).

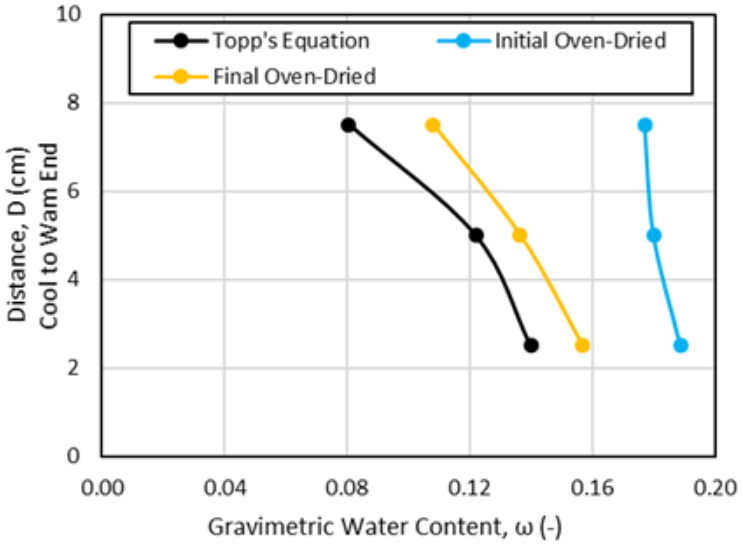

Figure 63. Nearly steady-state moisture distributions of ASTM fine sand (target ω = 18%).

4.4 References

Bach, L. (1992). “Soil water movement in response to temperature gradients: Experimental measurements and model evaluation.” Soil Sci. Soc. Am. J. 56:37-46.

Bouyoucous, G.T. (1915). “Effect of temperature on the movement of water vapor and capillary moisture in soils.” J. Agr. Res. 5:141-172.Cahill, Anthony T, and Marc B Parlange. 1998. “On Water Vapor Transport In Field Soils” 34 (4): 731–39.

Heitman, J. L., R. Horton, T. Ren, and T. E. Ochsner. 2010. “An Improved Approach for Measurement of Coupled Heat and Water Transfer in Soil Cells.” Soil Science Society of America Journal 71 (3): 872. https://doi.org/10.2136/sssaj2006.0327.

Jackson, Ray D. 1974. “Diurnal Changes in Soil Water Content During Drying.” https://doi.org/10.2136/sssaspecpub5.c3.

Prunty, L. and R. Horton. 1994. Steady-state temperature distribution in non-isothermal, unsaturated closed soil cells. Soil Sci. Soc. Am. J. 58:1358-1363.

CHAPTER V

SUMMARY AND CONCLUSIONS

5.1 Summary

Geothermal applications involve the use of geo-structures, such as ground-heat source pump (GSHP), which are geothermal systems operated to inject and extract underground heat for distribution to buildings and bridges. The effectiveness of these geo-structures depends in part on the soil surrounding them, since there is an interaction between the pipes that circulate heat and the underground unsaturated soil. Changes in soil temperature influence the migration of pore water from the soil and, in response, this movement alters the temperature of the soil. This coupled mechanism has been studied by several researchers and has been given the name of coupled thermo-hydro (TH) processes. This behavior has been explored both in the field and laboratory scale. This thesis focuses on the analysis of the coupled TH phenomenon of unsaturated soil in a laboratory setting using a modified double column-type testing device.

The new testing device comprises a modified configuration of its original design developed by previous researchers and includes various instrumentations to investigate one-dimensional heat transfer in unsaturated soil. It consists of a small and a larger column, with a heat exchanger at the top and at the bottom, alimented by a water bath circulator. The instrumentation includes thermocouples (TCs) and thermo-time domain reflectometry (T-TDR) and time domain reflectometry (TDR) sensors to measure the apparent dielectric constant (K_a) and bulk electrical conductivity (EC_b) of the soil. The measuring devices were partly manufactured and partly fabricated by the author with the assistance of colleagues, and the sensors were calibrated using different chemical substances to analyze their performance and obtain calibration equations.

Two types of sand, one consisting exclusively of sand particles (ASTM fine sand) and the other of both sand and finer particles (Hazy Meadow Park soil), were used for the laboratory investigations of the coupled TH behavior of unsaturated soil. Their gradation was determined, and they were tested for additional TDR calibration analyses. The selected soils were compacted in different molds for the determination of gravimetric water content (ω) using Topp's equation and a and b method, the estimation of calibration constants from One Step method, and the performance verification of the TDR sensors.

The soil samples were mixed with the desired moisture content, and the soil was compacted in the testing cell in four equal layers. The measuring devices were installed after each compacted layer. Following the compaction, the soil was allowed to equilibrate at 20ºC for a few hours. Assuming that the compacted soil had reached temperature equilibrium, temperature boundaries of 20ºC and 60ºC (for ASTM fine sand) and 20ºC and 40ºC (for Hazy Meadow Park soil) were imposed to the upper and lower heat exchangers for a period of 96 hours for temperature distribution. The temperature variations data were then collected, as well as the TDR waveforms of K_a and EC_b. The equipment was later dismantled, and soil samples were collected for water content determination, after the soil had reached equilibrium again.

The laboratory investigations were followed by the analysis of results and discussion. One-dimensional heat transfer was analyzed by observing the temperature profile between the top (cool region) and bottom (warm region) of the cell, having different temperature boundary conditions. Finally, the evaluation of the migration of water due to heat transfer and thermal gradients was carried out by determining the ω and temperature at each of the TDR sensors and TCs locations.

5.2 Conclusions

The conclusions that were drawn from the analysis of the laboratory investigations conducted and the results obtained are the following:

One-dimensional heat transfer was not perfectly achieved when no insulation was applied to the soil testing cell. The temperature profile of dry ASTM fine sand showed a slight sag at the middle of the cell, instead of the linear temperature profile described in the theory. Besides, the temperature profile of moist ASTM fine sand and Hazy Meadow Park soil displayed a concave downward temperature profile. This may have resulted in the lack of insulation in the soil testing cell, which could have impeded the ambient temperature of the test room to interact with the temperature distributed by the heat exchangers. The modified soil cell has however proved to maintain one-dimensional heat transfer when dry ASTM fine sand was tested with insulation. It was concluded that, if adequate insulation is provided, the modified soil testing cell has the ability to maintain one-dimensional heat transfer.

The coupled TH processes were most clearly observed for the Hazy Meadow Park soil with an initial ω of 6% and subjected to a thermal gradient of 200°C/m. This was due to the finer particles in the gradation of the Hazy Meadow Park soil, as the soil pore water adequately migrated from the warm end to the cool end, as predicted in the literature. This was less evident for the Hazy Meadow Park soil with an initial ω of 10%. For ASTM fine sand, however, the pore water sank to the bottom, causing little or no movement of the pore water from the warm end to the cool end. Additionally, the modest magnitude of thermal gradient (200°C/m for Hazy Meadow Park soil against 400°C/m for ASTM fine sand) may have played an important role in the migration of Hazy Meadow Park soil pore water. It was then concluded that unsaturated soil samples with the largest

quantity of fine particles, in addition to a relatively low initial moisture content and a moderate temperature gradient, more correctly exhibit the coupling behavior of TH processes.

5.3 Recommendations

This section provides a list of recommendations that could improve the laboratory investigations and analyses conducted to study the coupled TH processes of unsaturated soil.

1. Firstly, it would be highly recommended to provide proper radial insulation to the modified soil cell, so as to avoid the interference of the ambient temperature and to fully achieve one-dimensional heat transfer for dry and moist unsaturated soil.

2. It would also be necessary to test supplementary soil samples of different grain sizes, with various moisture content and several thermal gradients to corroborate the findings of this thesis that the size of grains, initial moisture content, and the magnitude of thermal gradient are the most important factors that influence the migration of moisture in unsaturated soil.

3. Extensive calibration analyses should also be carried out to better examine the performance of TCs, TDR, and T-TDR sensors.

4. A final recommendation would be to evaluate additional soil parameters and thermal properties, i.e., matric suction and thermal conductivity, to better determine the volumetric and gravimetric water content of soil.